

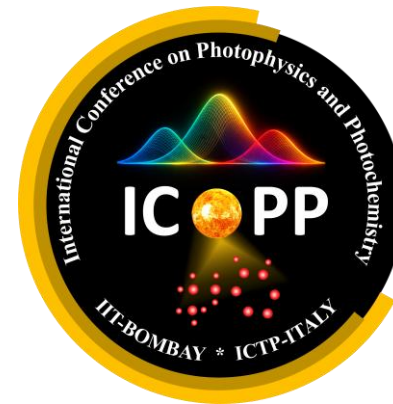
Optical and Charge Transport Properties of Halide Perovskite Nanocrystals for Multifunctional Devices



Samit K. Ray

Department of Physics, IIT Kharagpur

email: physkr@phy.iitkgp.ac.in

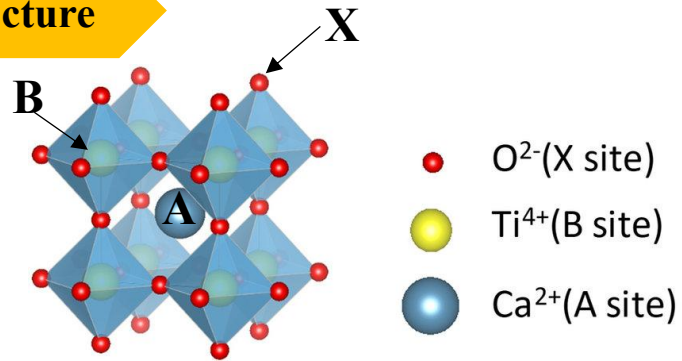


Funding support :

- IMPRINT (MHRD & DRDO)
- NNETRA, INUP (Meity)
- DST- ANRF, Nanomission

*ICOPP 2026
IIT Bombay, March 28th, 2026*

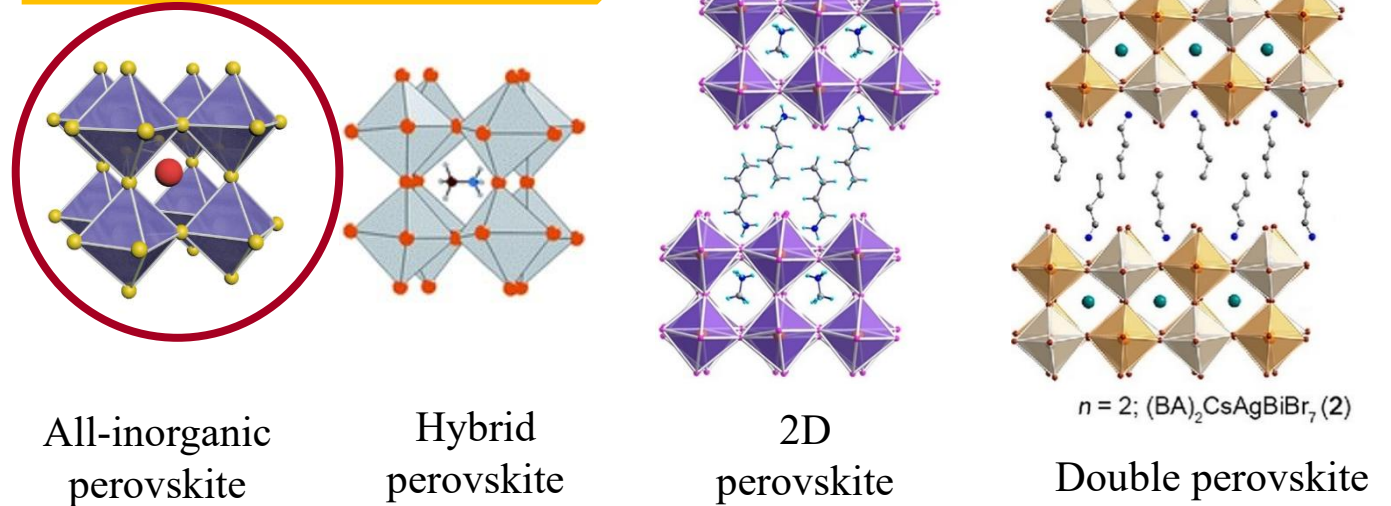
Structure



General form of perovskites: ABX_3

$A = Cs^+, MA^+, FA^+$
 $B = Pb^{2+}, Sn^{2+}, \text{etc.}$
 $X = Cl^-, Br^-, I^-$

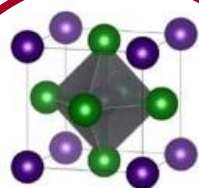
Different types of perovskites



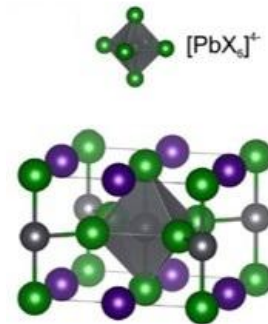
ACS Energy Lett. 2021, 6, 8, 2750–2754

Phases of perovskites

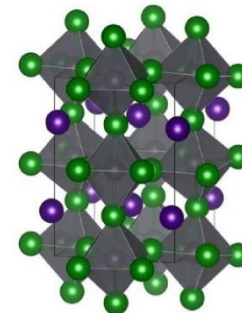
● $A = Cs^+/MA^+/FA^+$
● $X = Cl^-/Br^-/I^-$



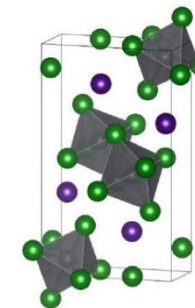
Cubic (α)



Tetragonal (β)

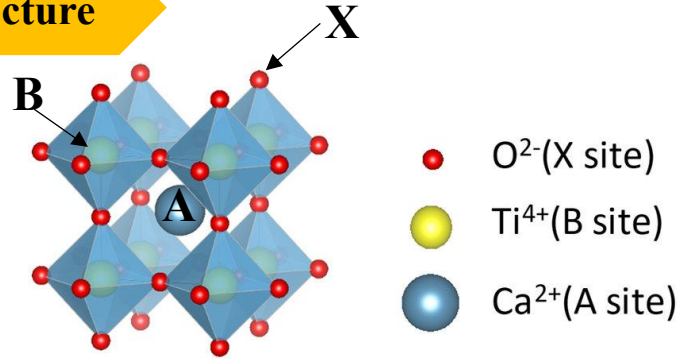


Orthorhombic (γ)



Non-perovskite (δ)

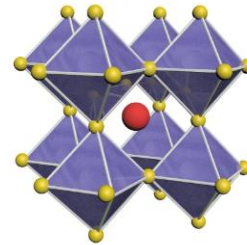
Structure



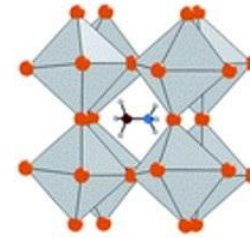
General form of perovskites: ABX_3

$A = Cs^+, MA^+, FA^+$
 $B = Pb^{2+}, Sn^{2+}, etc.$
 $X = Cl, Br, I^-$

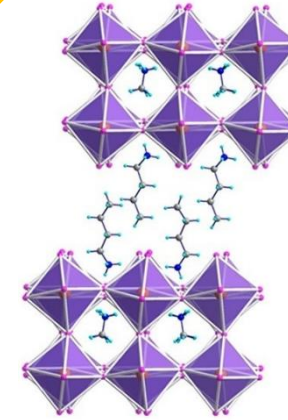
Different types of perovskites



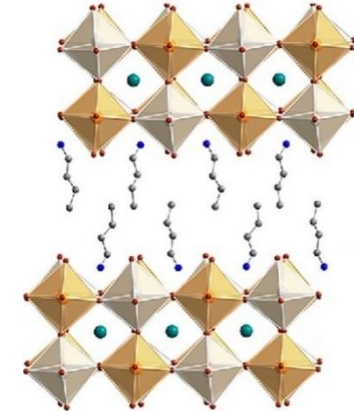
All-inorganic perovskite



Hybrid perovskite



2D perovskite



$n = 2; (BA)_2CsAgBiBr_7(2)$
 Double perovskite

ACS Energy Lett. 2021, 6, 8, 2750–2754

Properties

- Exceptional electroluminescence (near unity quantum yield)
- High absorption coefficient ($\alpha \sim 10^5 \text{ cm}^{-1}$)
- Tuneable band gaps ($\sim 1.7 \text{ eV} - 2.5 \text{ eV}$)
- Inexpensive fabrication methods

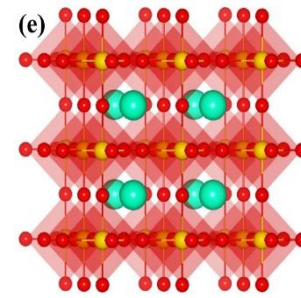


RESEARCH ARTICLE

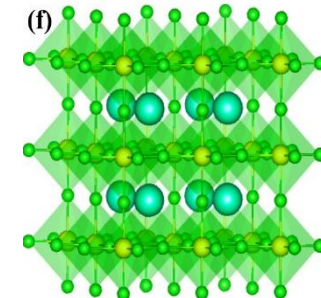
ADVANCED
FUNCTIONAL
MATERIALS
www.afm-journal.de

Atomic Insights of Stable, Monodispersed CsPbI_{3-x}Br_x (x = 0, 1, 2, 3) Nanocrystals Synthesized by Modified Ligand Cell

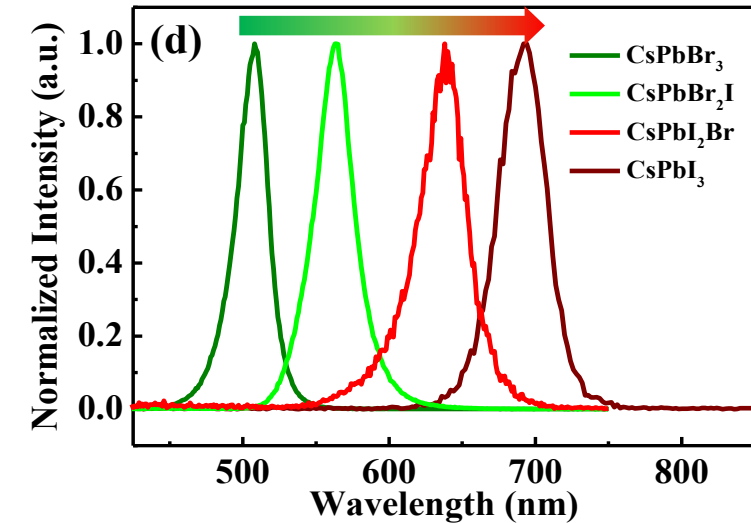
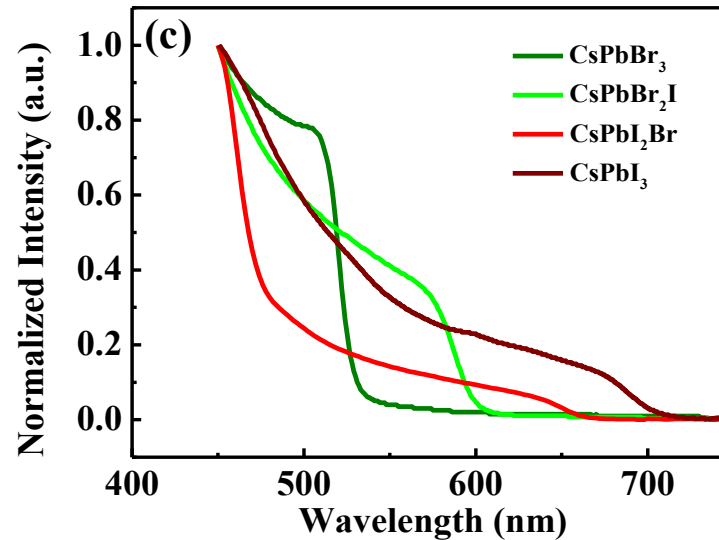
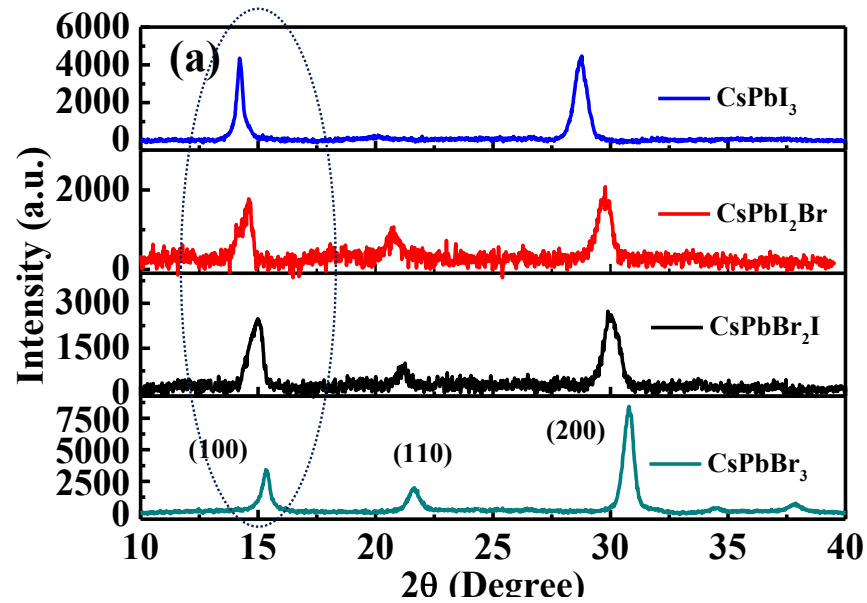
Arup Ghorai, Somnath Mahato,* Sanjeev Kumar Srivastava, and Samit K. Ray*



CsPbI₃



CsPbBr₃



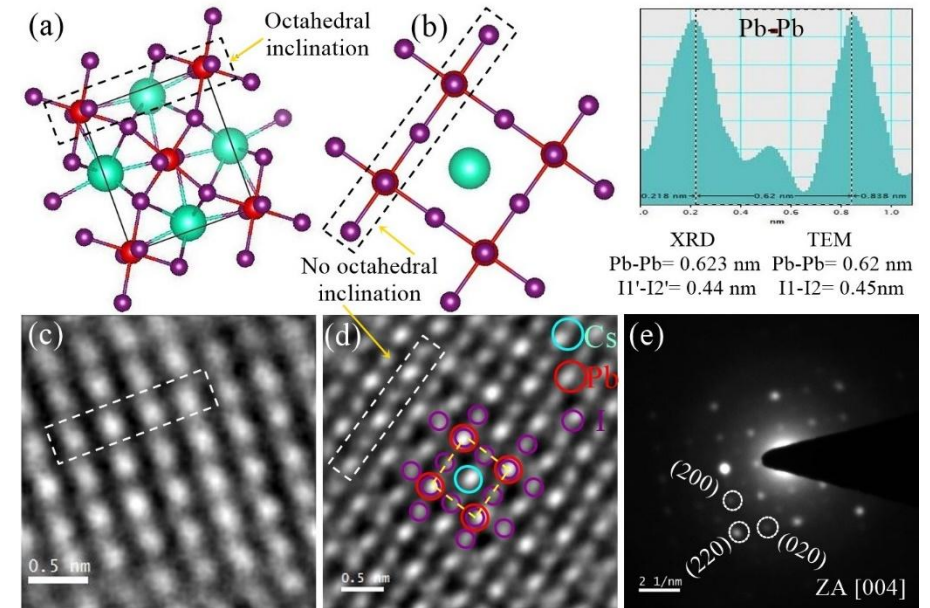
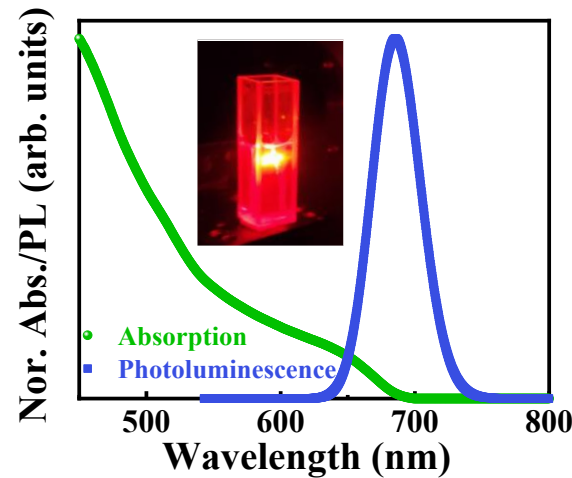
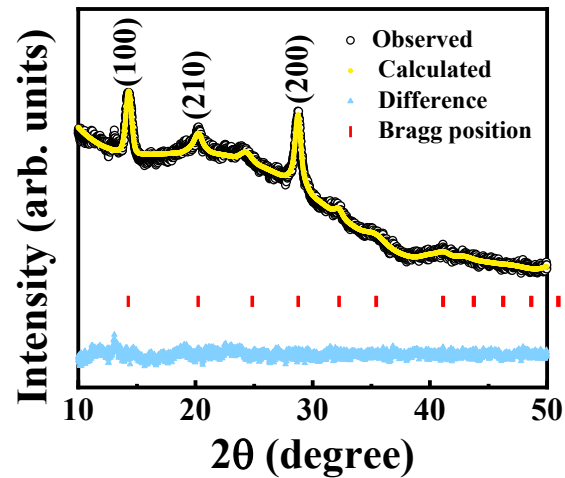
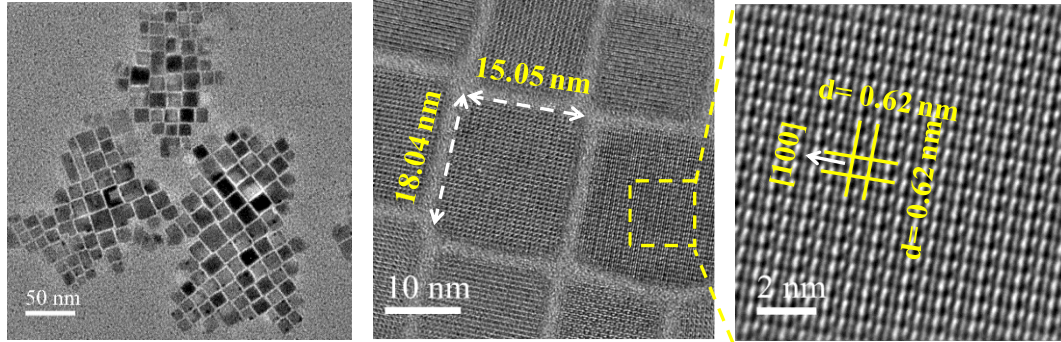
Gradual red shift in absorption and photoluminescence peaks with increase in iodine



Halide Perovskite Nanocrystals

- Cubic α -CsPbI₃ : High stability using oleyl amine as a ligand
- Smaller lattice constant : $a=6.2315\text{\AA}$

Chemically synthesized of α -phase CsPbI₃ NCs



Atomic positions of Cs, Pb and I

- Structural and optical characteristics of as-synthesised CsPbI₃ NCs : Cubic α -phase formation with extended visible photoabsorption up to 700 nm

Mahato et al., Advanced Energy Materials, 2001305, (2020)
 Ghorai et al., Advanced Functional Mater, 2202087 (2022)
 Ghorai et al., Angewandte Chemie, 135, e202302852 (2023)

Bose et al., Appl. Phys. Lett. 124, 011901 (2024)
 Mahato et al., Advanced Materials, e03680 (2025)



Talk Outline

I. CsPbI₃ Nanocrystals Sensitized Optoelectronic Devices

- High performance phototransistors
- Nanocrystal sensitized photovoltaic devices

II. Halide Perovskite : Optical & Neuromorphic Devices

- Mixed halide perovskites Light emitting diode (LED) : Effect of R-P faults
- Doping & interface engineered optical synaptic devices

Attempted way to improve device stability

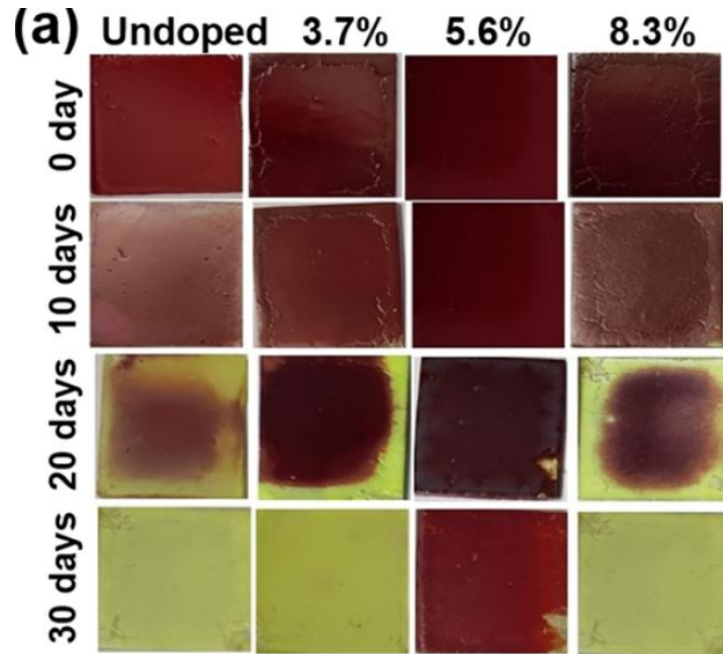


I. B-site Doping

Goldschmidt's tolerance factor

$$\tau = \frac{r_A + r_B}{\sqrt{2}(r_B + r_X)}$$

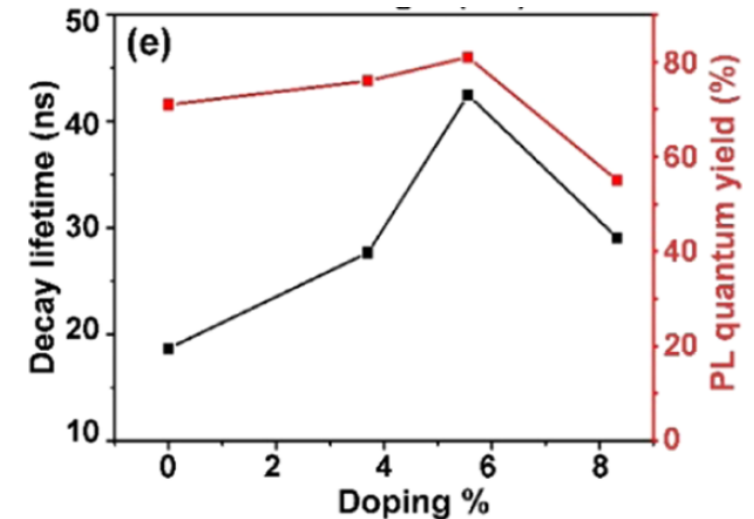
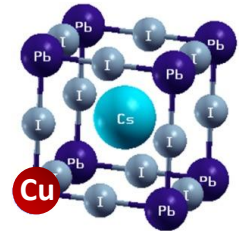
r_A , r_B , and r_X = effective ionic radii of the A-, B-, and X-site atoms of perovskites (ABX_3)



- Doping 5.6% Cu results in maximum enhancement in structural stability of metal halide perovskite $CsPbI_3$
- Film stable for more than 30 days in ambient conditions
- Radiative decay lifetime and photoluminescence yield increases for 5.6% Cu-doping

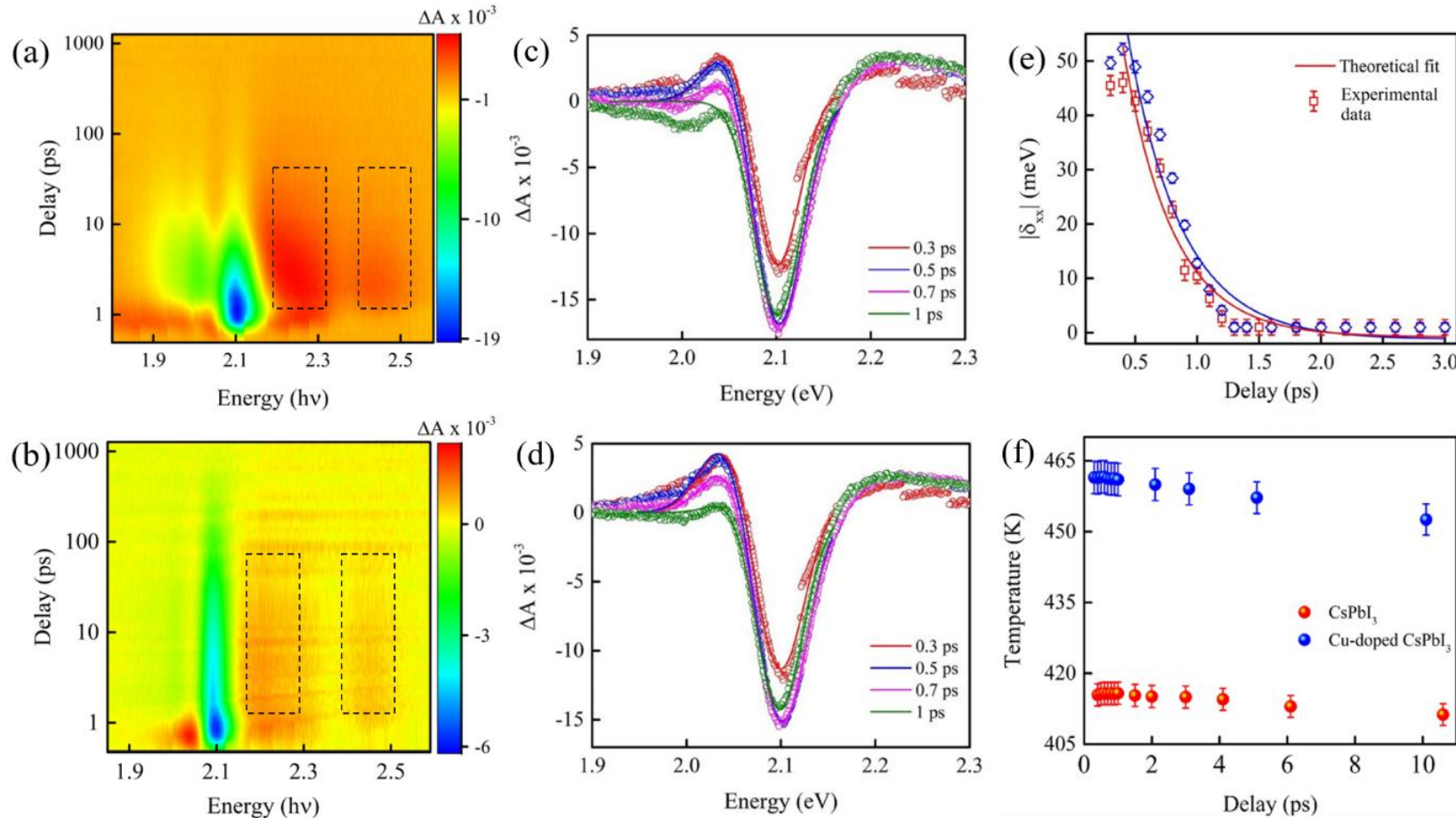
- Ideally, $\tau \sim 1$
- For $CsPbI_3$, $\tau \sim 0.893$

Cu, $t \sim 0.98$



Roy et al., Chemistry of Materials, 1601 (2023)

Improvement in hot carrier dynamics



Doping enhances hot carrier energy and thermalization time : suitable for hot-carrier perovskite solar cells

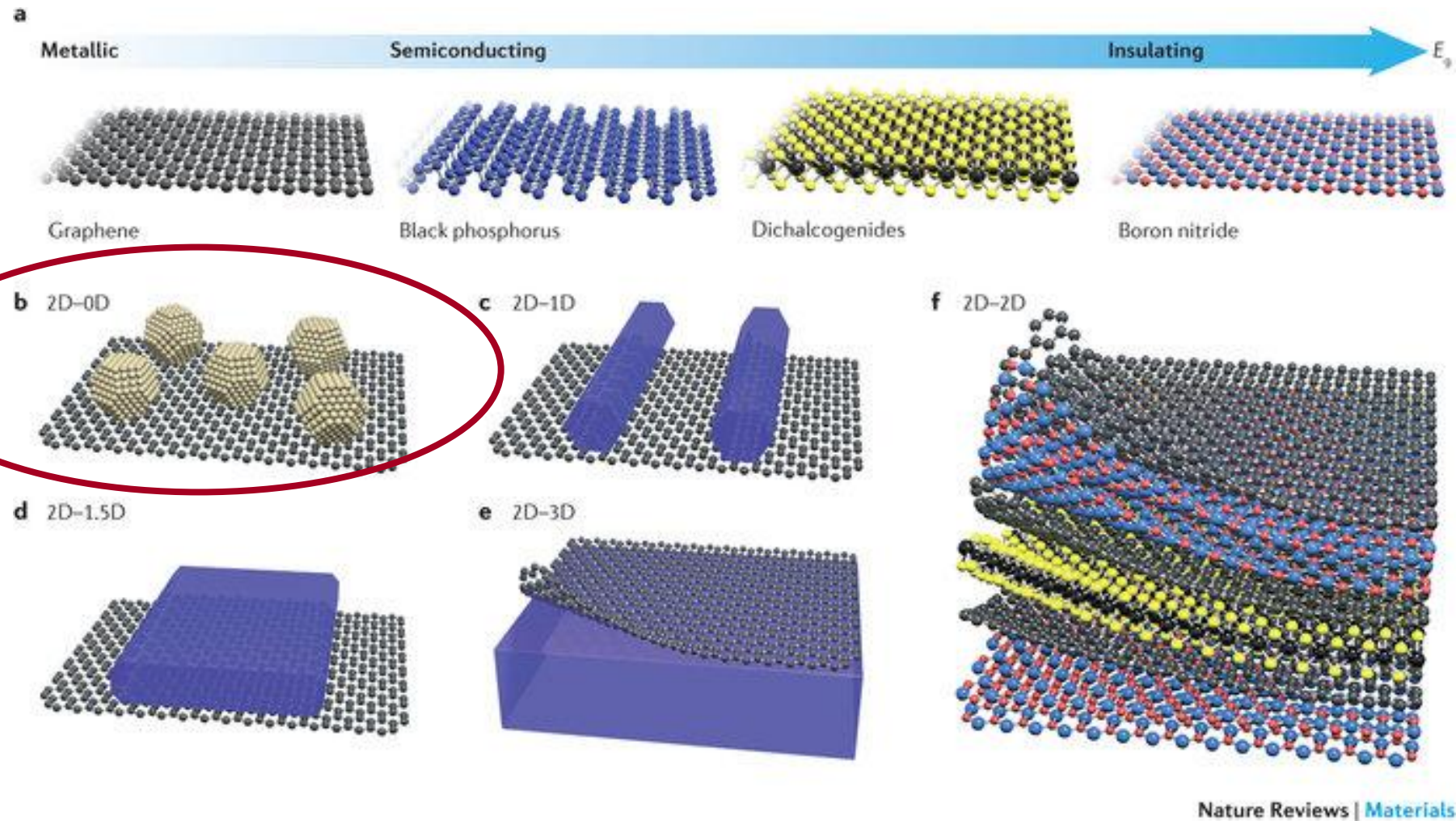
In collaborations with K.V.Adarsh, IISER Bhopal

Bose et al., *Appl. Phys. Lett.* 124, 011901 (2024)

TA spectrum at a peak intensity of 15 μJ/cm² for 3.1 eV pump excitation of (a) undoped and (b) Cu-doped CsPbI₃ NCs. Selected cross-section of the contour plots of TA spectrum at Δt ≤ 1 ps for (c) undoped and (d) Cu-doped CsPbI₃ NCs. (e) Biexcitonic shift calculated at different delay times for undoped and Cu-doped CsPbI₃ NCs. (f) Carrier temperature: At time, Δt < 1 ps, carriers at ~461 K and ~415 K for doped system and CsPbI₃, respectively.



Mixed-dimensional Heterostructures

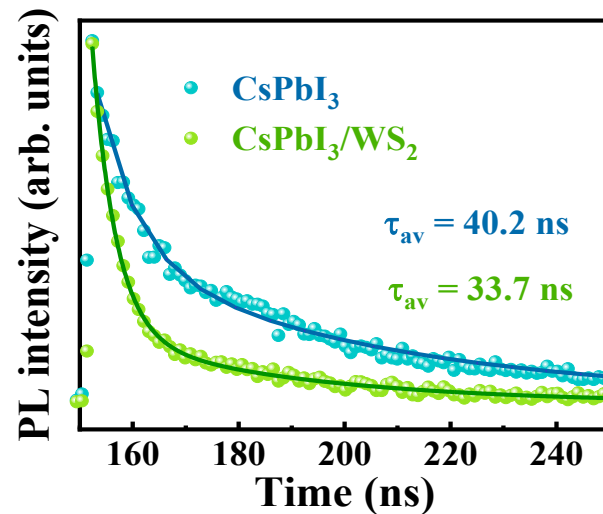
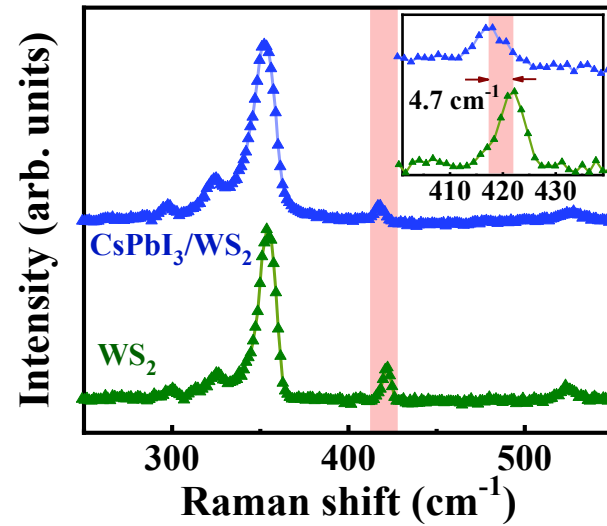
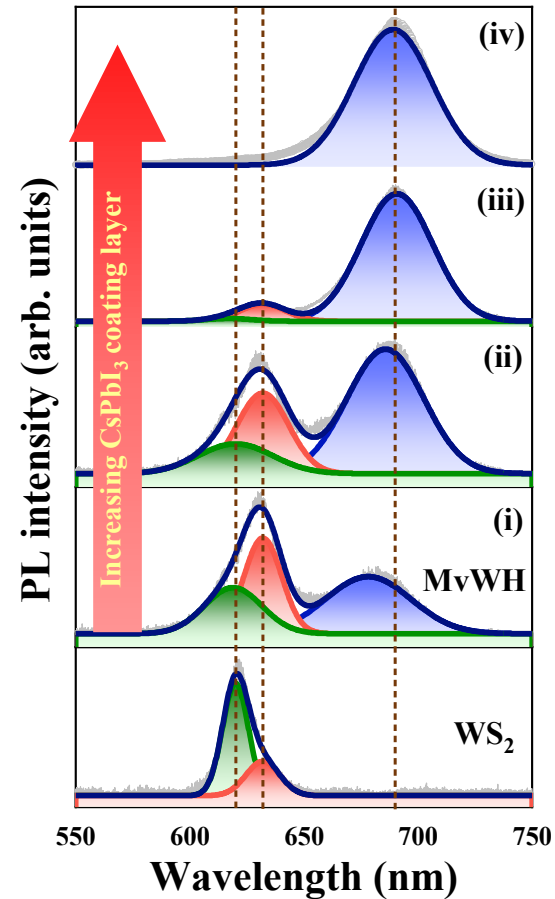


Achieve 2D/nD Heterostructures for Si-CMOS Compatible Photonic Applications

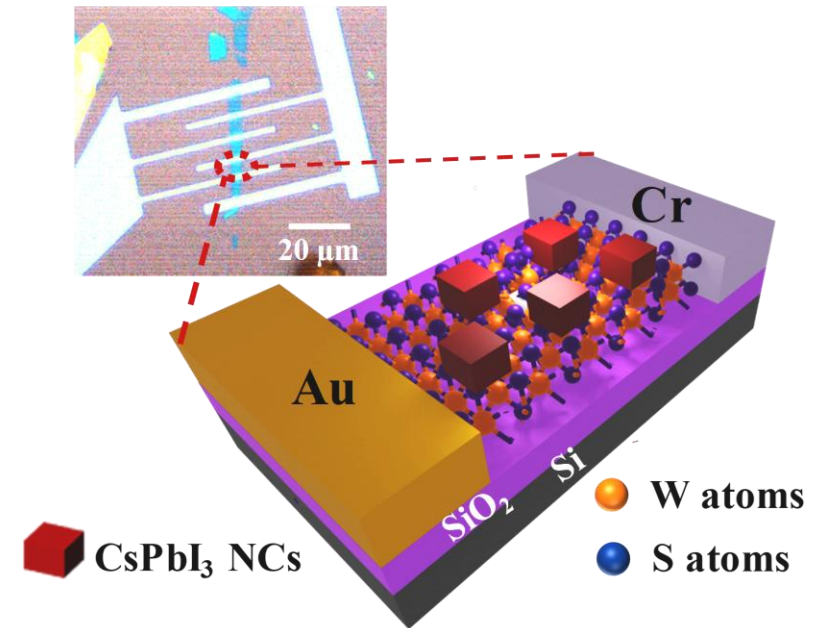


I. CsPbI₃ NCs/WS₂ (0D/2D) Heterojunction Phototransistor

Charge transfer mechanism in heterostructure samples



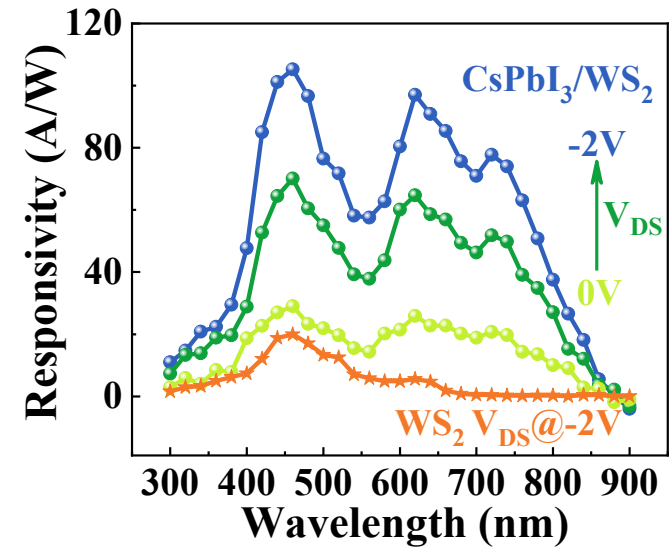
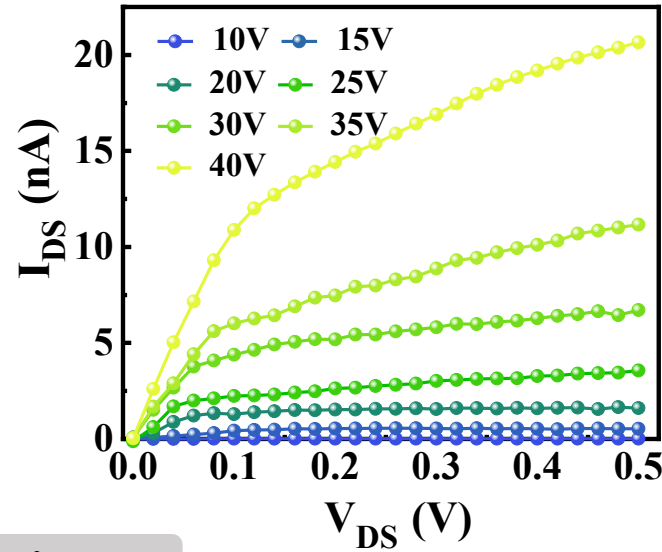
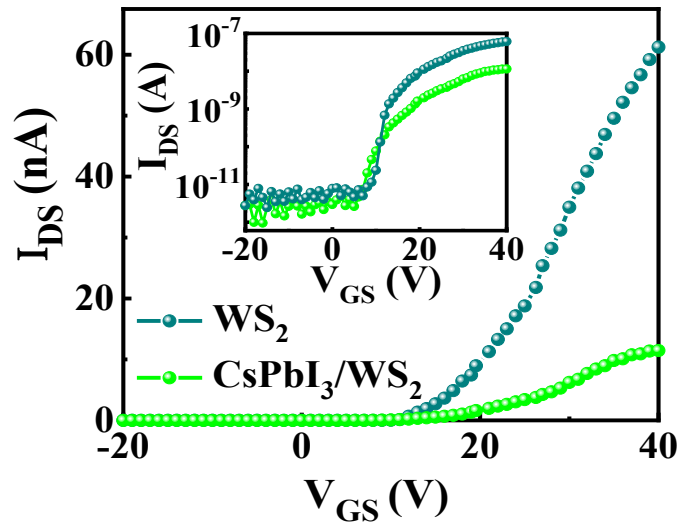
- WS₂ excitonic peak quenches
- WS₂ trionic peak enhancement
- Overall CsPbI₃ PL peak quenches



Das et al., Physical Review Applied 19.3 (2023): 034051.



QDs Sensitized WS₂ Phototransistor with asymmetric contacts



Photoresponse characteristics

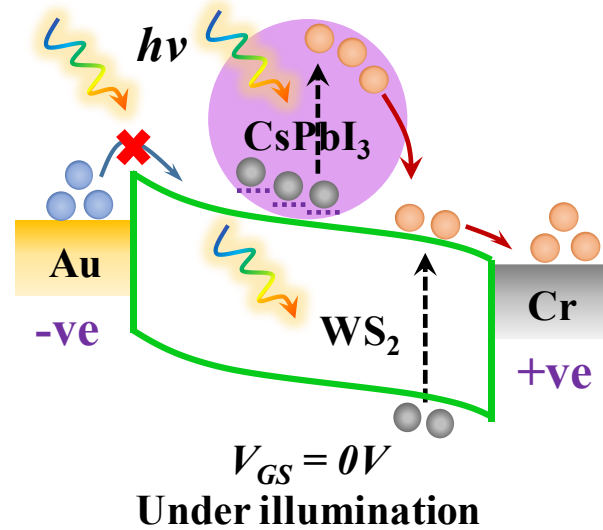
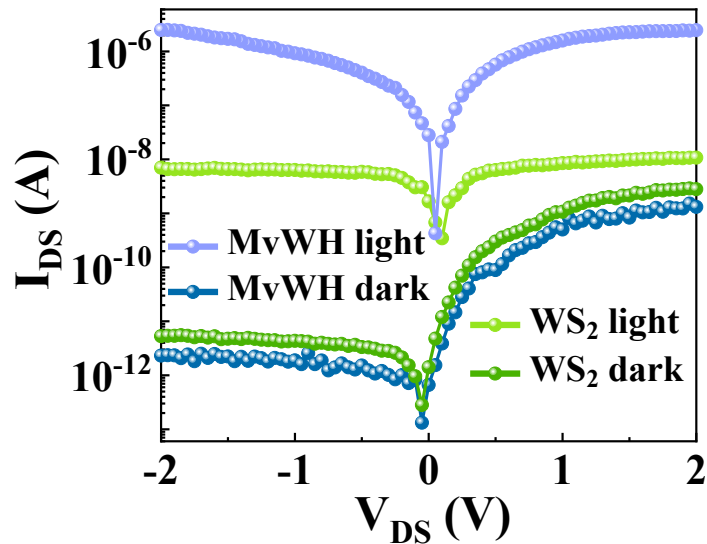


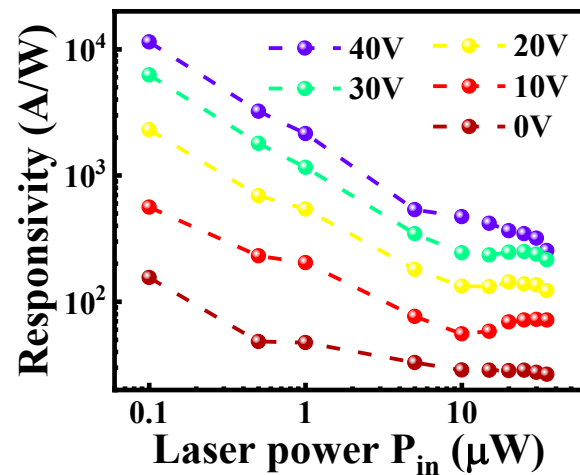
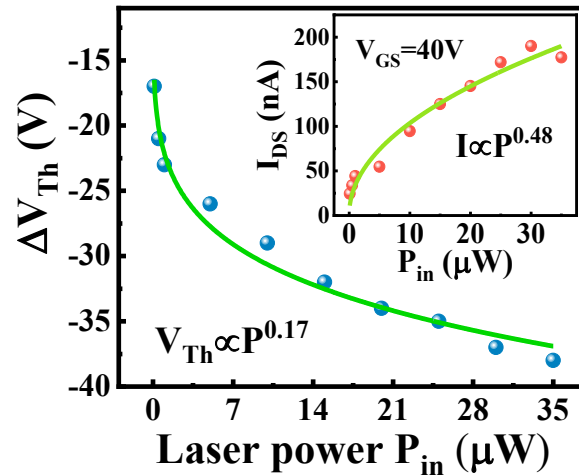
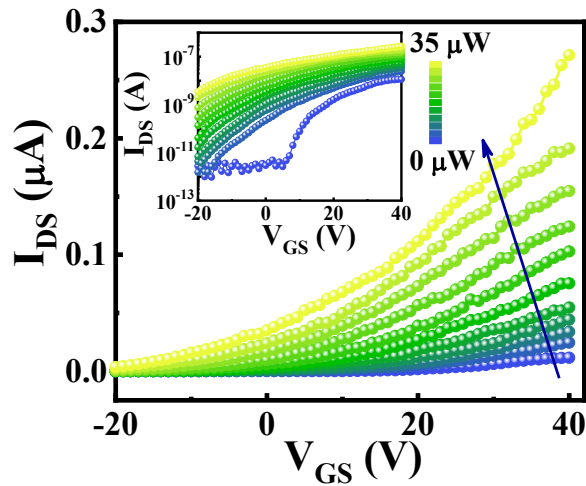
Photo-FET at zero gate bias: Enhanced & extended spectral response up to 900 nm

Photo-to-dark current ratio: $\sim 10^6$ for CsPbI₃/WS₂



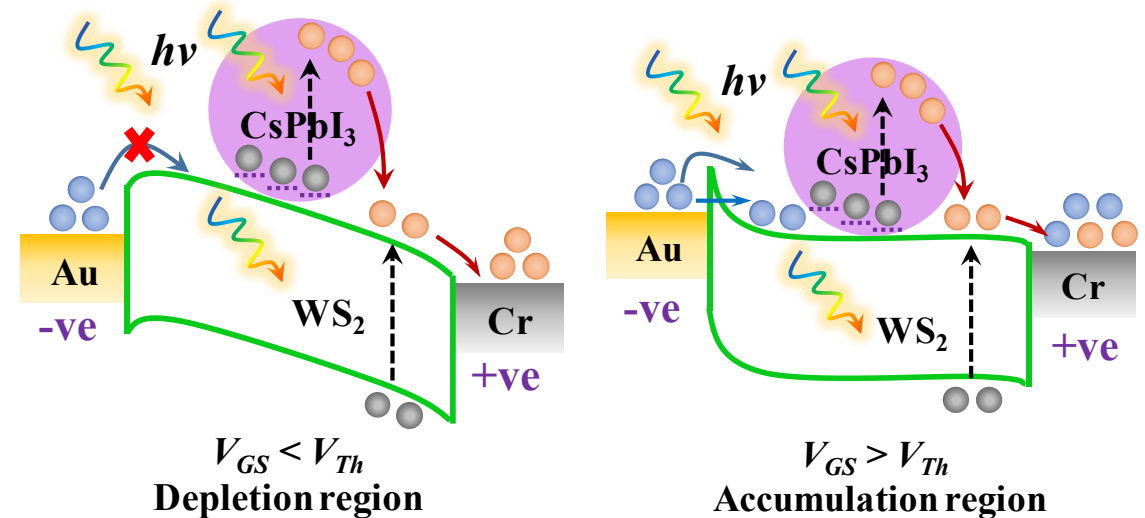
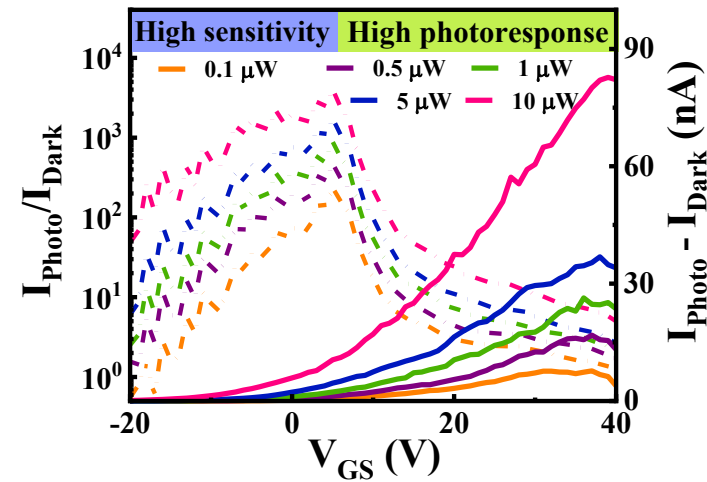
Gate tunable phototransistor characteristics

Strong photo gating effect from trapped holes inside CsPbI₃ NC sensitizers



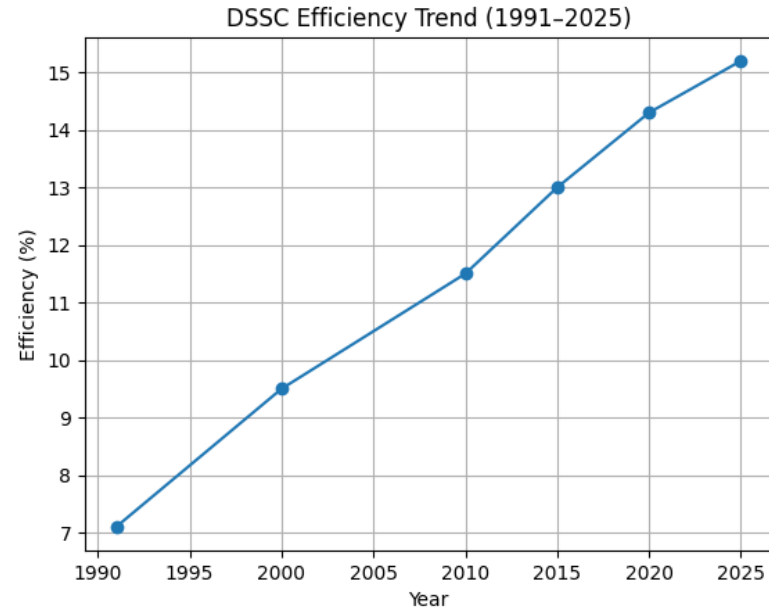
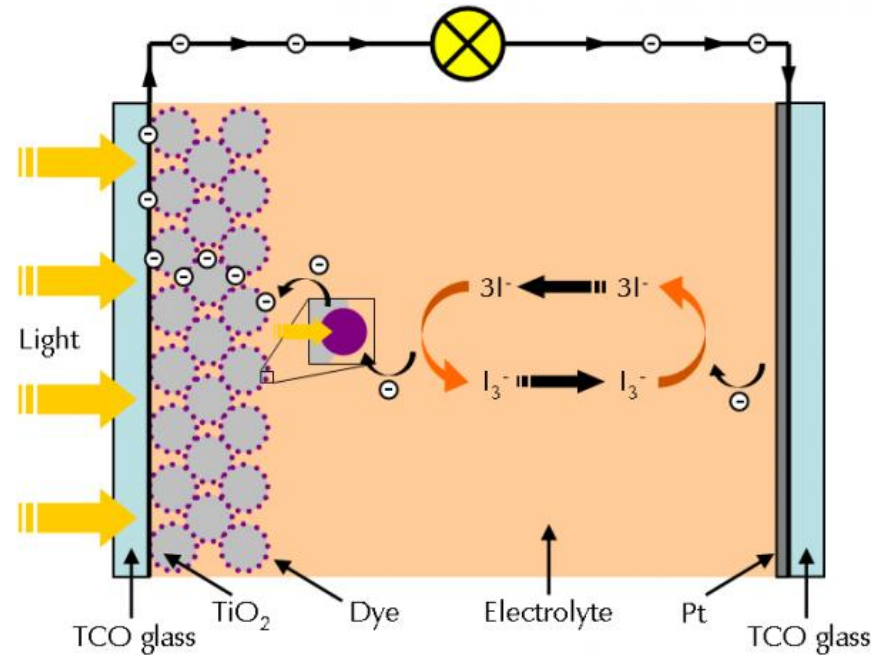
- The maximum responsivity $\sim 10^4$ A/W at $V_{GS}=40$ V
- The detectivity is $\sim 1.2 \times 10^{13}$ Jones.

Gate tunable photo-FET performance: from high sensitivity to high photoresponse





II. Perovskite NCs Sensitized PV Devices



Limitations of DSSCs :

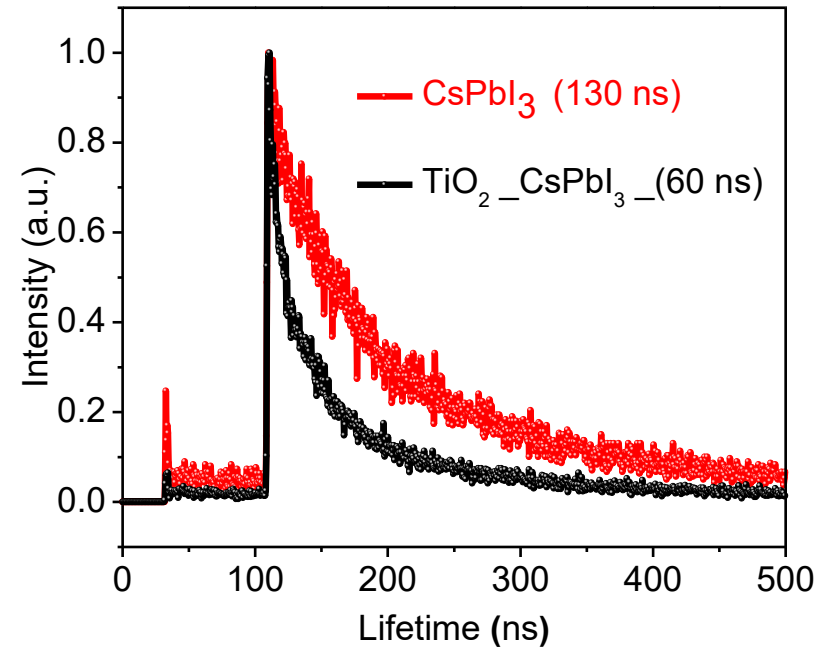
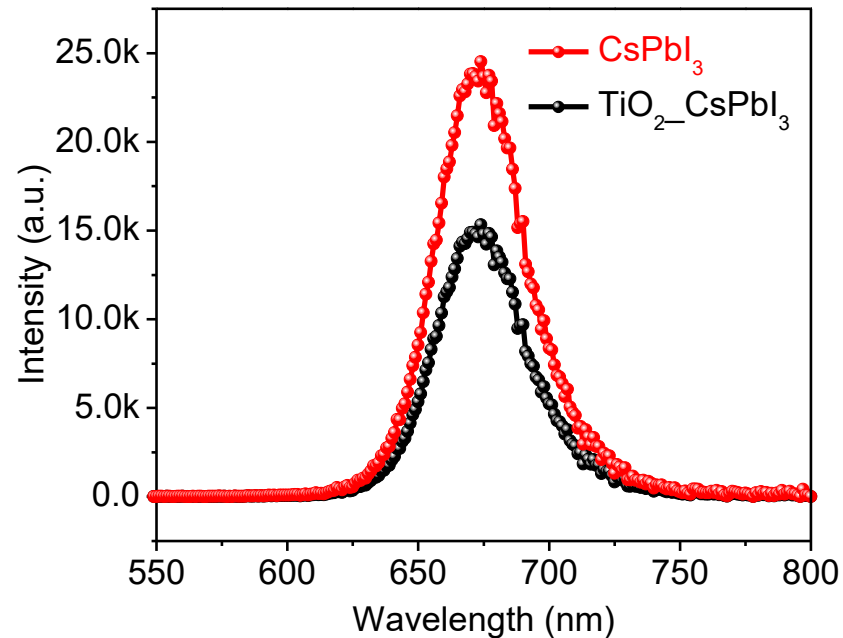
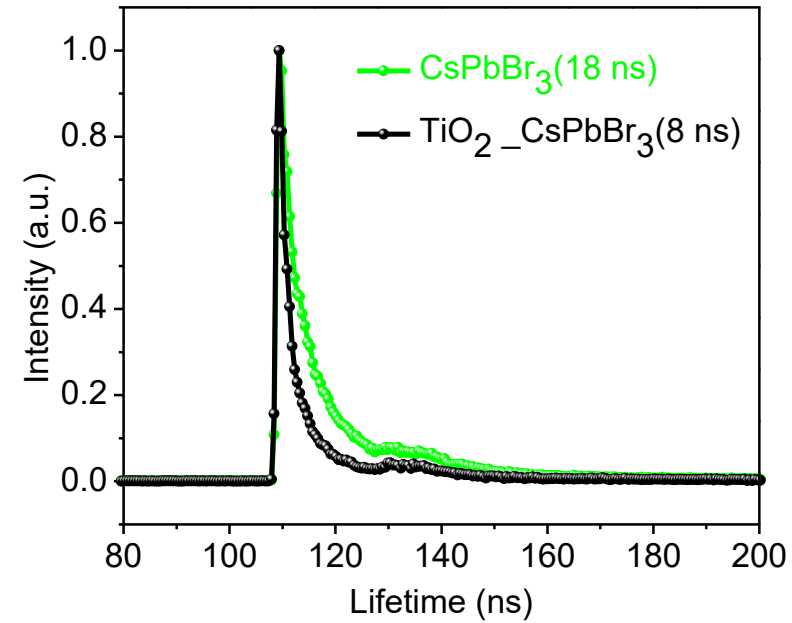
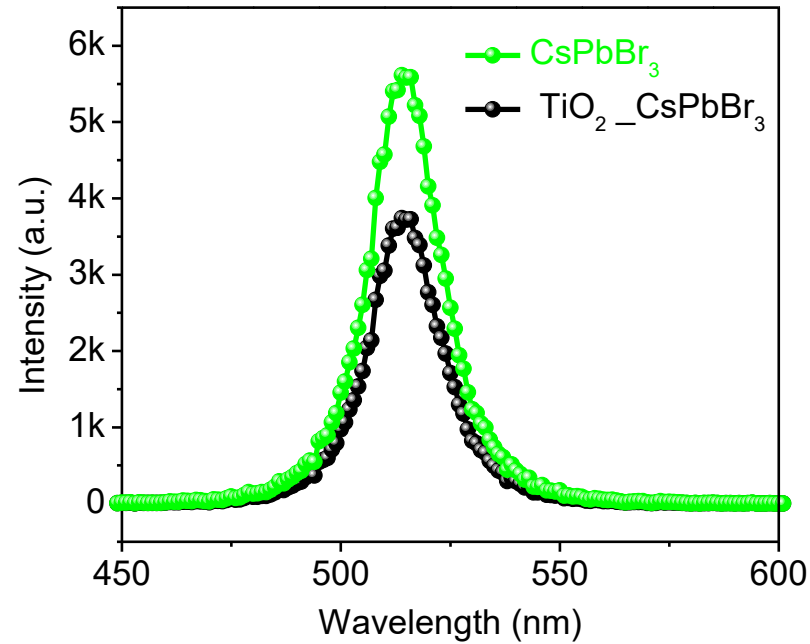
- ❑ Dyes degrade under UV and prolonged light exposure
- ❑ Dye molecules can aggregate on TiO₂ surface
- ❑ Slow electron injection
- ❑ Structural changes reduce performance

Nanocrystal Sensitizers :

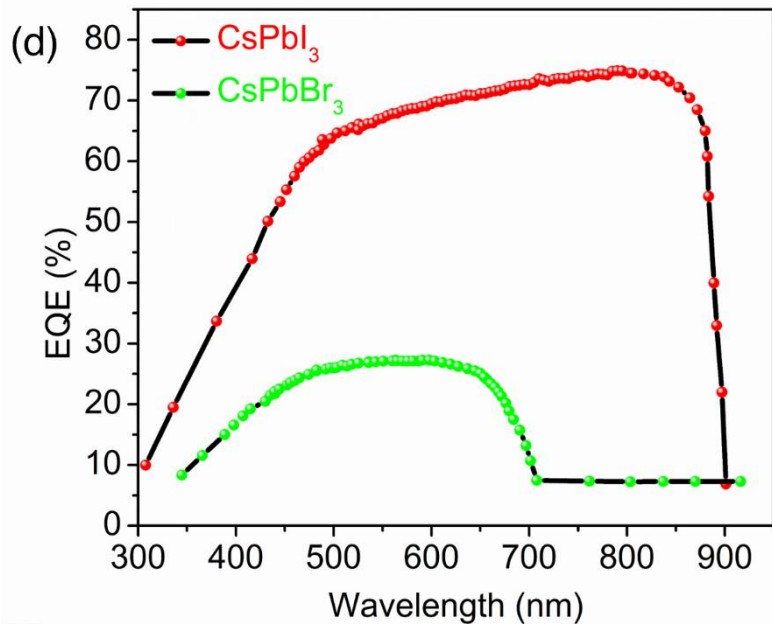
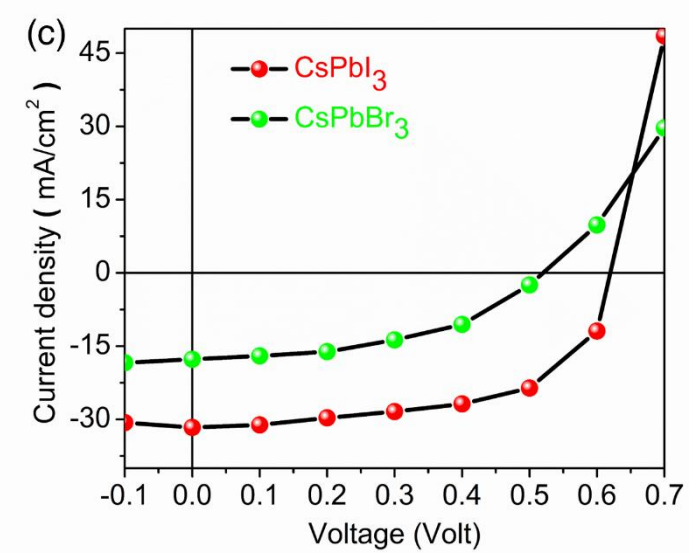
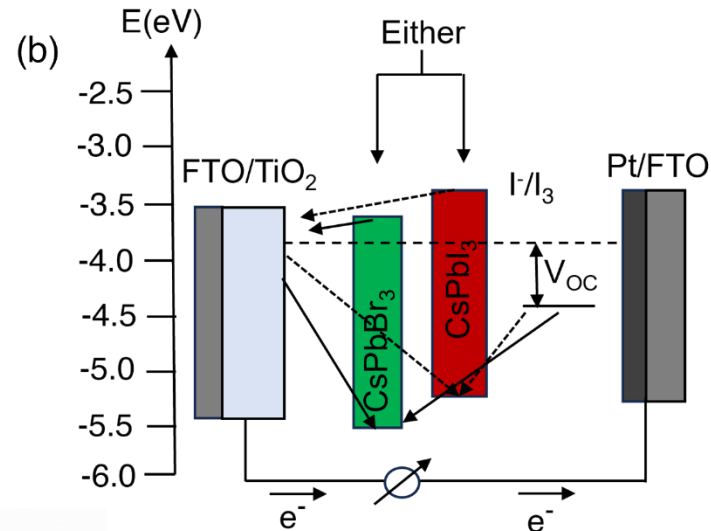
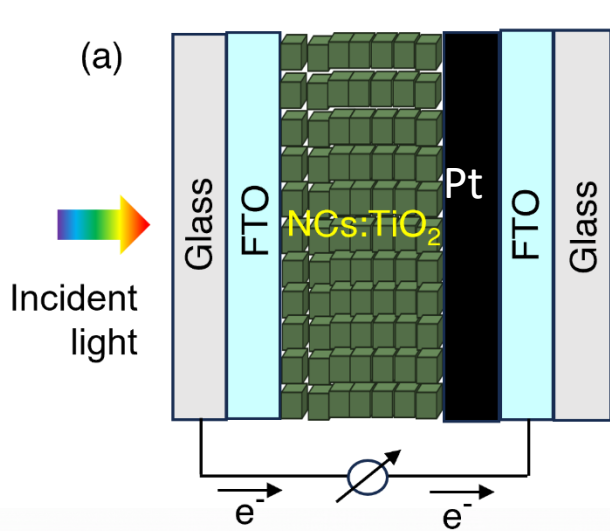
- ❑ Higher absorption coefficient ($\sim 10^5 \text{ cm}^{-1}$)
- ❑ High carrier mobility and long diffusion lengths ($\sim 1 \mu\text{m}$)
- ❑ Tunable bandgap (1.2–2.3 eV) by changing halides (I, Br, Cl)



Perovskite NCs Sensitizers

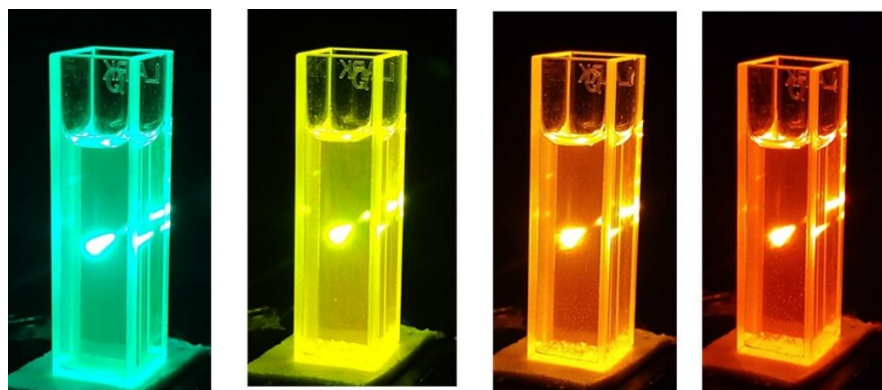
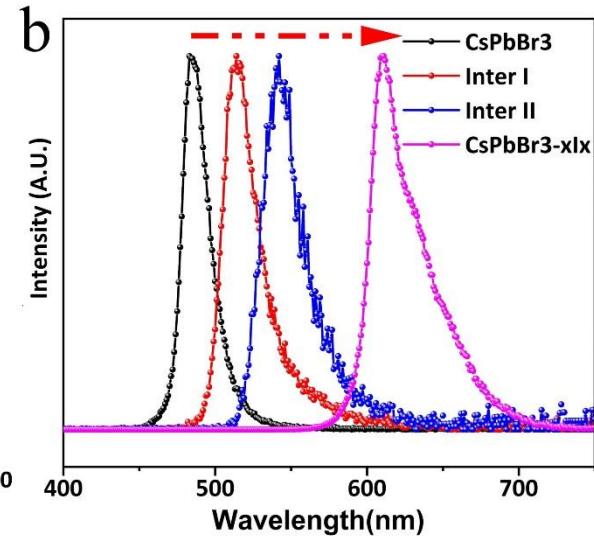
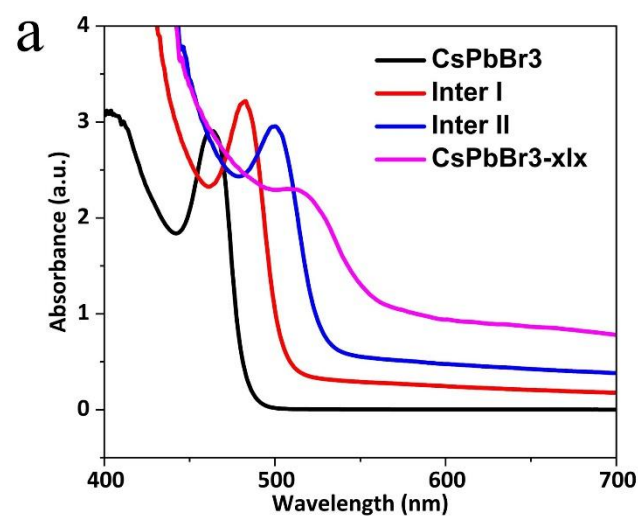
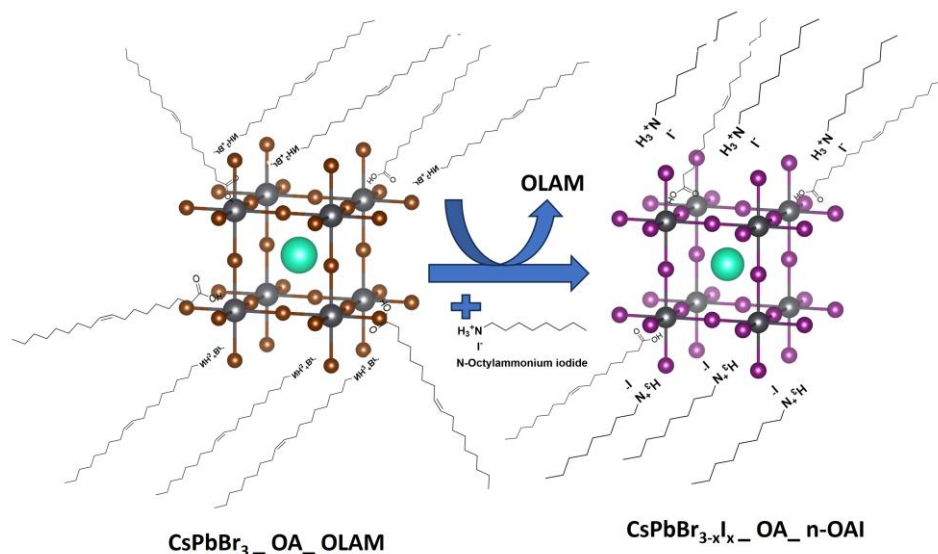


Perovskites NCs-sensitized solar cells



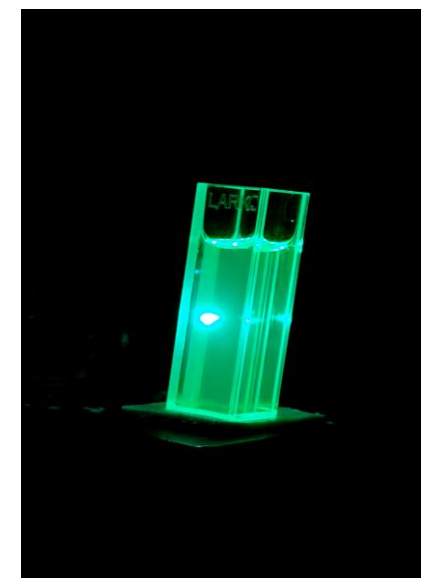
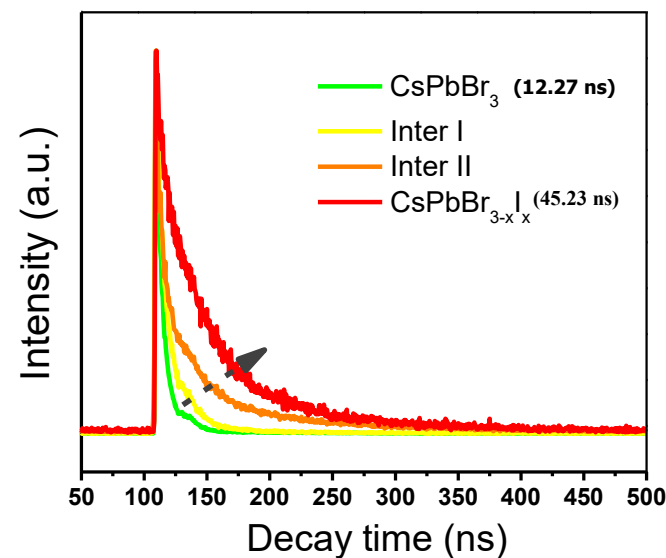
Active materials	J _{sc} (mA/cm ²)	V _{oc} (V)	FF (%)	PCE (%)
CsPbBr ₃	18.1	0.52	42	3.9 %
CsPbI ₃	32.1	0.61	64	12.5 %

III. Anion Exchanged Mixed Halides : LEDs



$\text{CsPbBr}_{3-x}\text{I}_x$

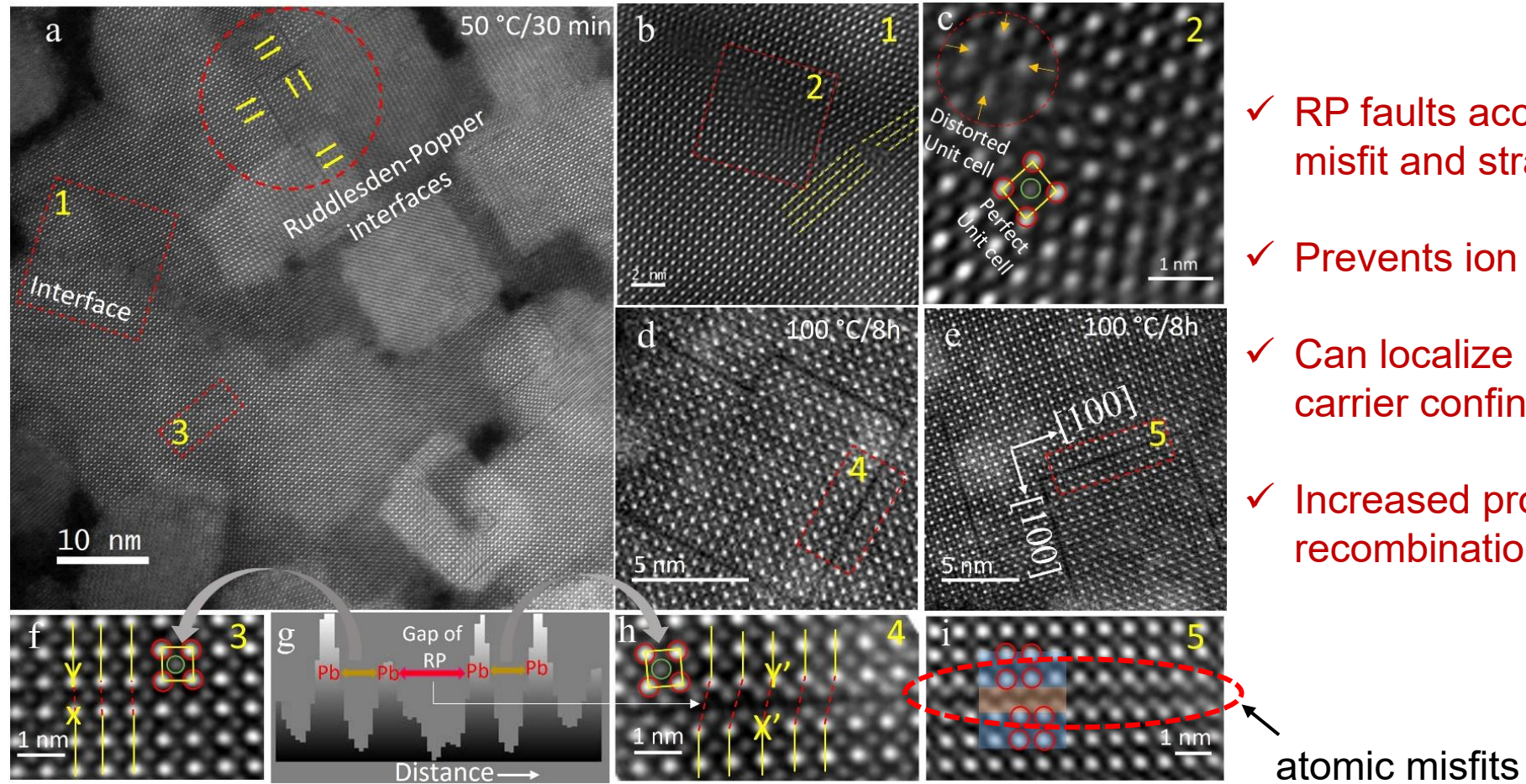
n-octylammonium Iodide



Video of CsPbBr_3
to $\text{CsPbBr}_{3-x}\text{I}_x$

MHPs : 2D Ruddlesden - Popper (RP) Faults

HAADF-STEM images of ligand-treated CsPbBr₃



- ✓ RP faults accommodate misfit and strain
- ✓ Prevents ion migration
- ✓ Can localize carriers – carrier confinement
- ✓ Increased probability of recombination

From flaws to functional assets : RP faults for light emission

Perovskite-info
3PATAT-C3
Efficient Charge Recovery from Perovskite Layer

PHYS ORG
Topics
Nanotechnology Physics Earth Astronomy & Space Chemistry Biology Other Sciences

Researchers turn flaws in perovskite crystals into functional assets

In the world of materials science, defects are usually seen as problems, unwanted microscopic features that degrade performance, reduce efficiency, and shorten the life span of devices. But a recent study by scientists from the European Research Network – Polish Centre for Technology Development and Indian Institute of Technology Kharagpur challenged this perception.

1
f
Twitter
Share
Email

Home / Chemistry / Analytical Chemistry
Home / Chemistry / Materials Science

AUGUST 11, 2025
Rethinking imperfections: How defects are powering brighter perovskite emissions
by Somnath Mahato and Muhammad Danang Birowosuto
edited by Lisa Lock, reviewed by Robert Egan

RESEARCH ARTICLE
ADVANCED MATERIALS
www.advmat.de

Atomically Precise Ruddlesden–Popper Faults Induced Enhanced Emission in Ligand Stabilized Mixed Halide Perovskites

Somnath Mahato,* Baidyanath Roy, Shaona Bose, Satayender K. Sangwan, Narayan Chandra Das, Muhammad Danang Birowosuto, and Samit K. Ray*

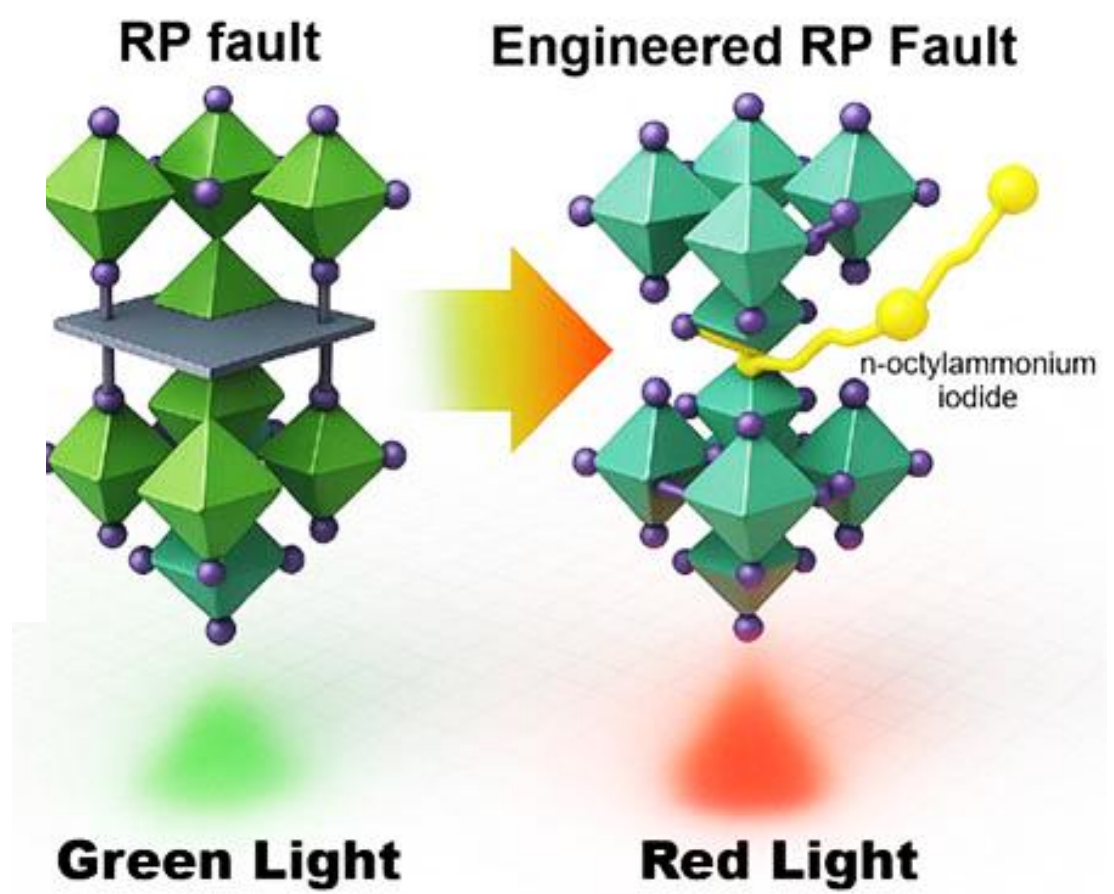
MEDIA NEWS

When flaws become features: Turning defects into brighter perovskite emission

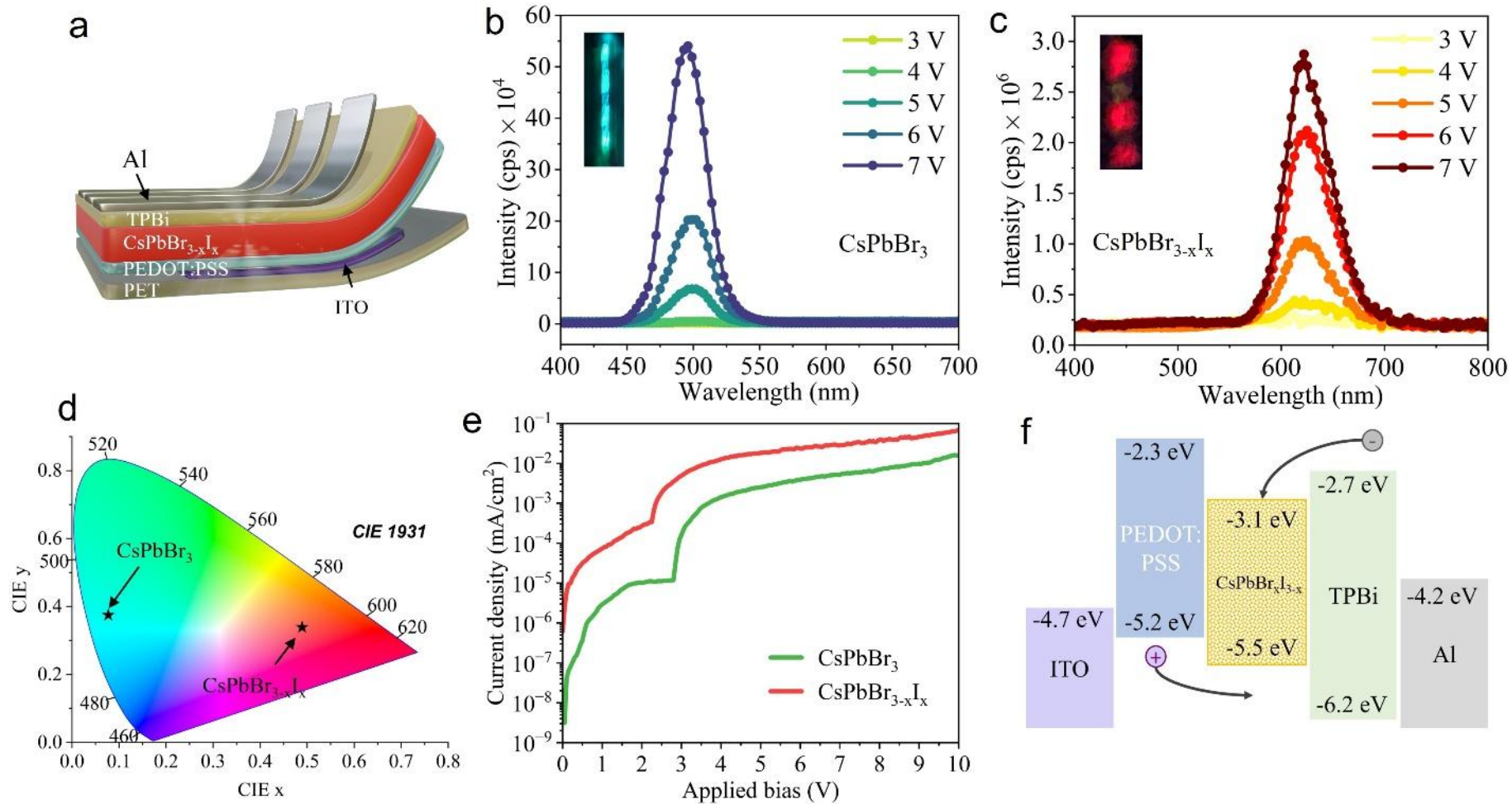
Engineered atomic faults in perovskites boost light emission by nearly 80 percent and improve stability, offering new design strategies for brighter, more durable optoelectronic devices.

(Nanowerk News) In the world of materials science, “defects” are usually the bad guys, tiny imperfections in a material’s structure that sabotage performance, drain efficiency, or shorten a device’s life span. But a new study published in *Advanced Materials* (“Atomically Precise Ruddlesden–Popper Faults Induced Enhanced Emission in Ligand Stabilized Mixed Halide Perovskites”) flips this idea on its head. It reveals how a long-misunderstood defect in crystals, known as the Ruddlesden–Popper (RP) fault, could be the secret ingredient to unlocking brighter and more stable light-emitting materials.

At the heart of this discovery are perovskites, a family of materials making waves for their use in solar panels, LEDs, lasers, and even quantum technologies. Perovskites are prized for their unique crystal structures, which allow electrons and other charge carriers



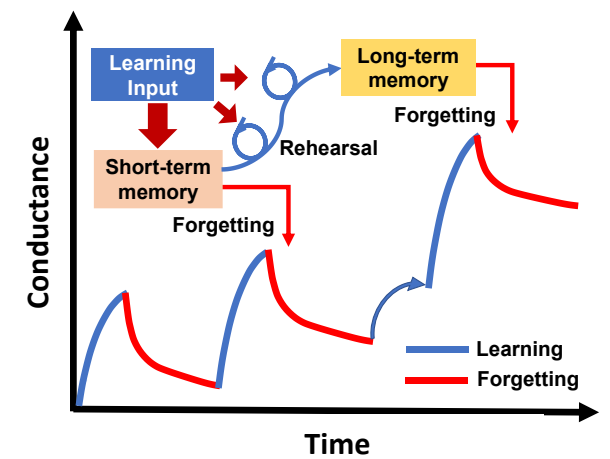
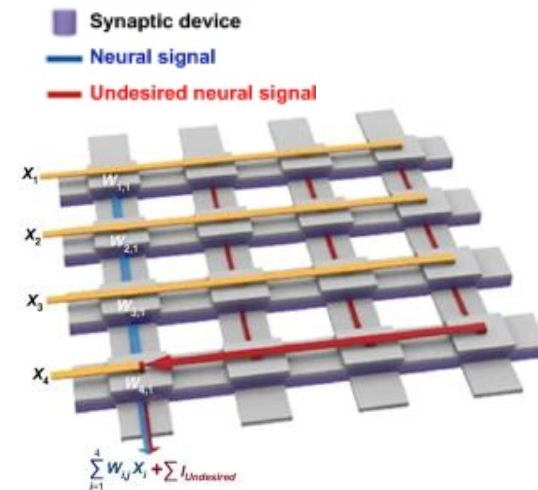
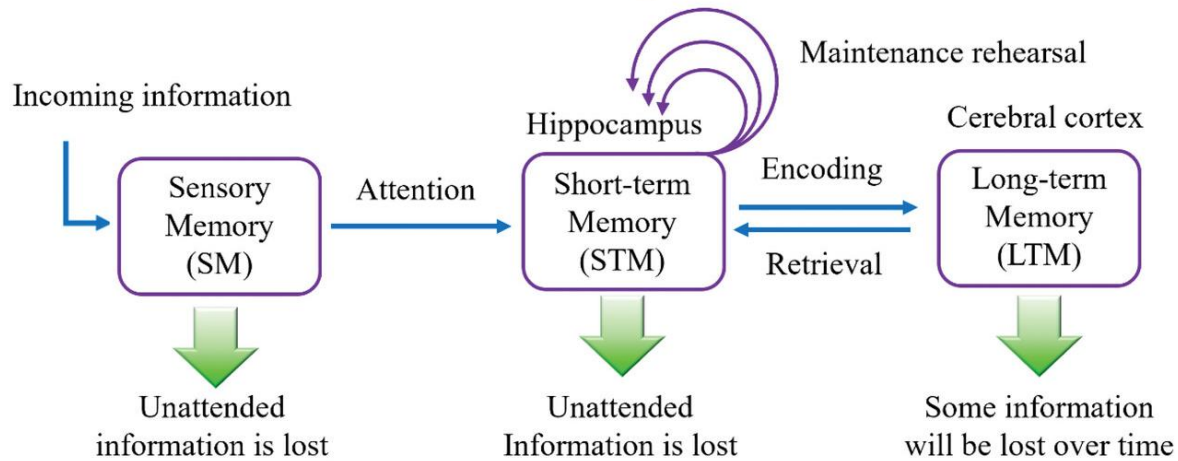
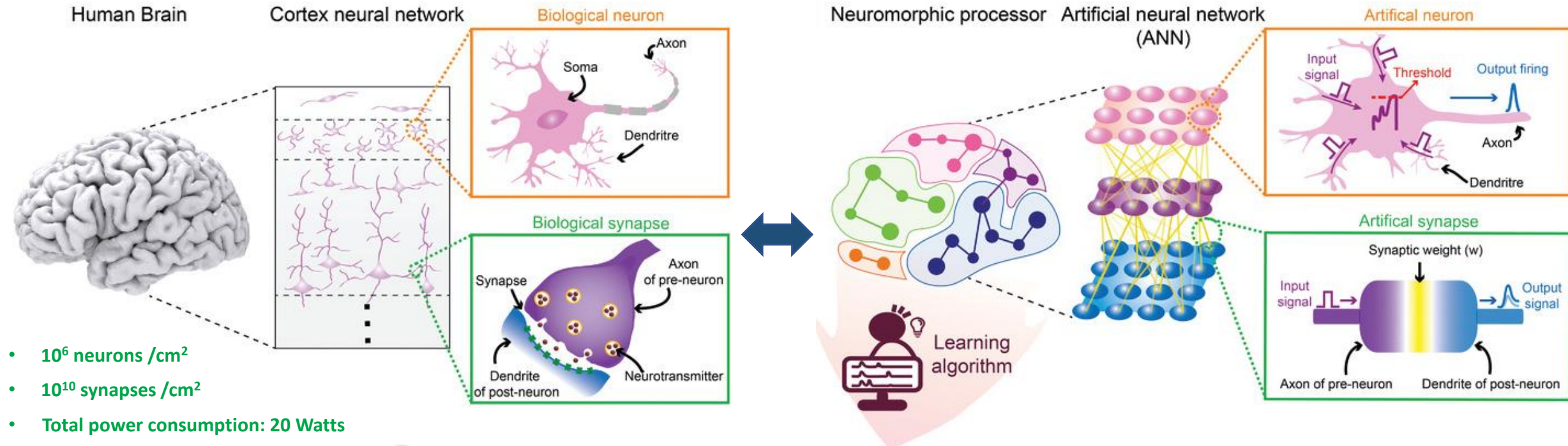
LEDs : Using NOAI-induced RPFs



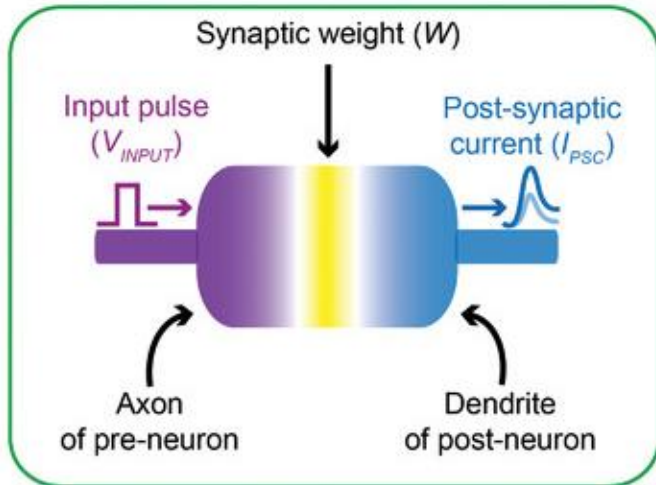
Electroluminescence intensity increased by 80%!



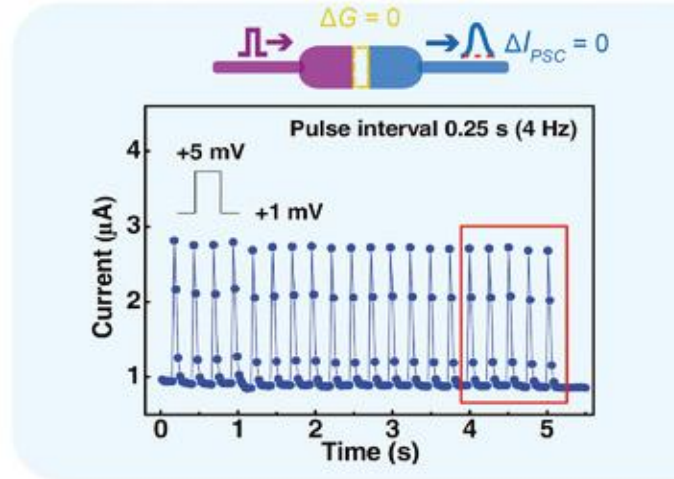
IV. Brain-inspired (Neuromorphic) Devices



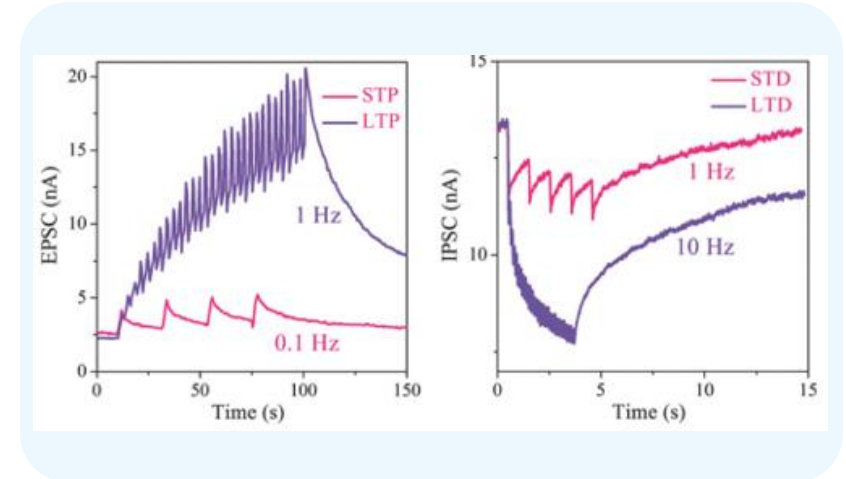
Representative synaptic functions



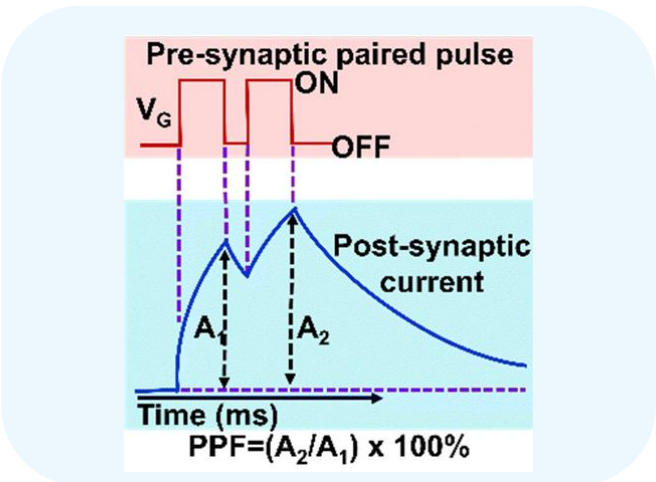
Short-term plasticity (STP)



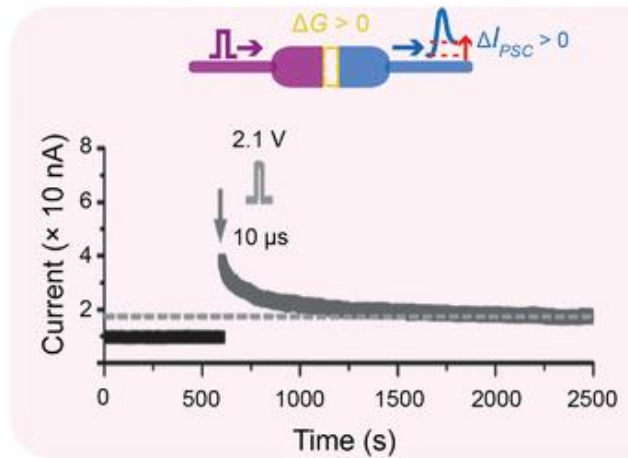
Spike rate-dependent plasticity (SRDP)



Paired pulse facilitation (PPF)



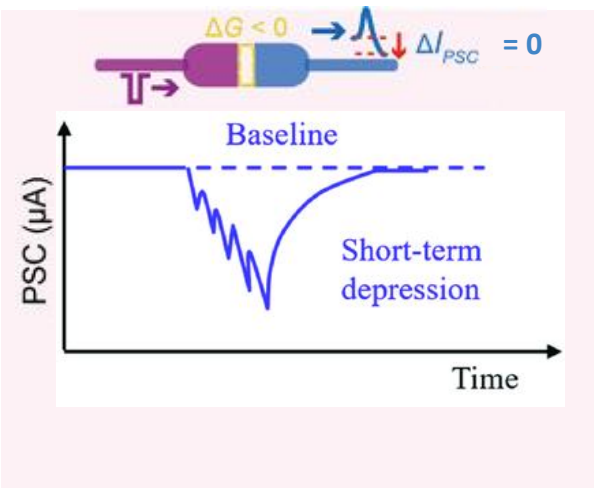
Long-term potentiation (LTP)



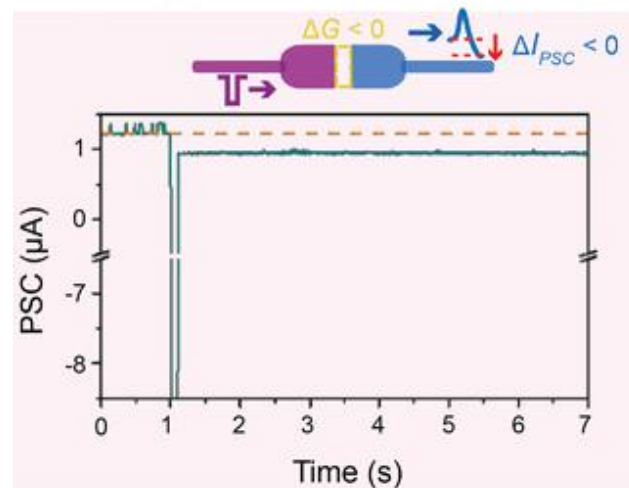
- ❖ **Synaptic weight regulation:** Increase in synaptic weight (potentiation) and decrease in synaptic weight (depression)
- ❖ **Short-term plasticity:** Temporal increase of synaptic weight
- ❖ **Long-term potentiation:** Permanent change in synaptic weight
- ❖ **Spike rate-dependent plasticity:** Synaptic weight variance as a function of spiking rate
- ❖ **Paired pulse facilitation (PPF):** Current changes between the adjacent pulses.

Essential Functions of Artificial Synapses

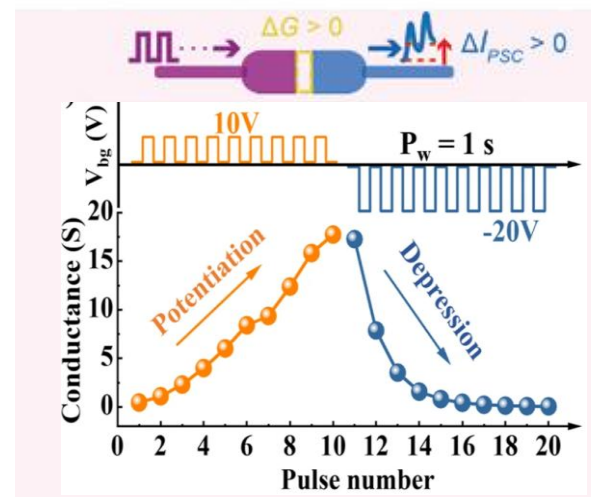
Short-term depression (STD)



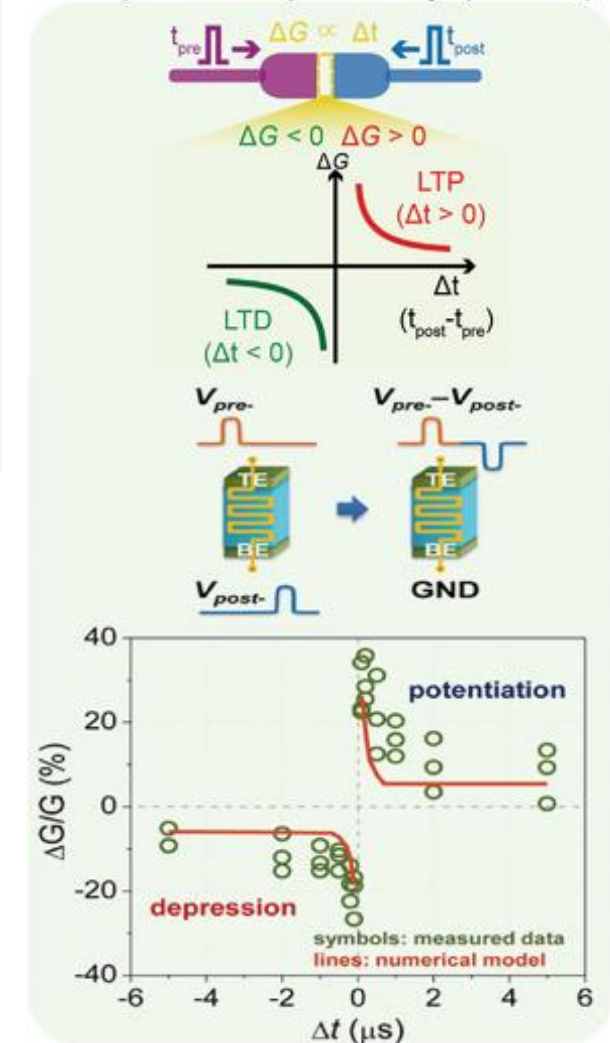
Long-term depression (LTD)



Consecutive LTP & LTD



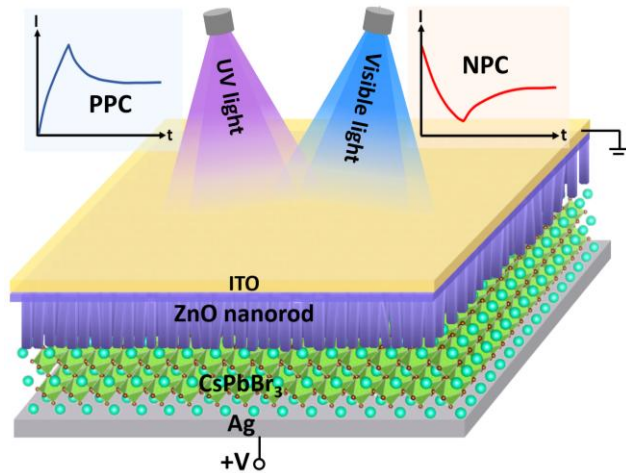
Spike-timing dependent-plasticity (STDP)



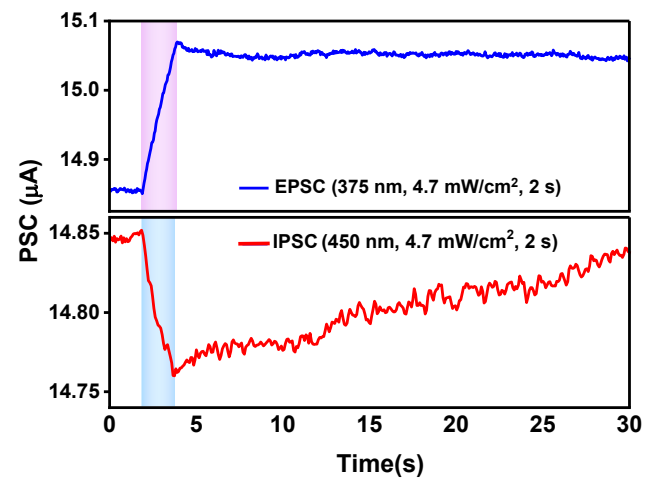
- ❖ **Short-term depression (STD):** Temporal decrease of synaptic weight
- ❖ **Long-term depression (LTD):** Permanent low value of synaptic weight
- ❖ **Consecutive LTP and LTD:** This emulation can be controlled by a pulse train consisting of potentiating and depressing pulses, causing an analog change in the synaptic weight.
- ❖ **Spike timing-dependent plasticity (STDP):** Synaptic weight variance as a function of spiking time difference between the firing of the pre- and post-synaptic neurons.



Bidirectional Photoresponse in Perovskite/Oxide Heterojunction

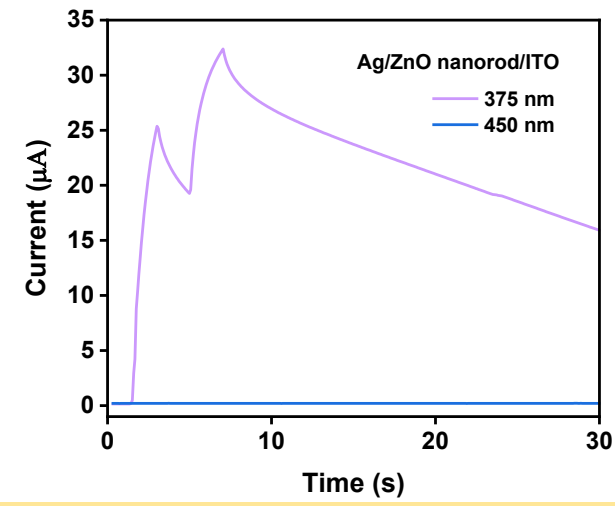
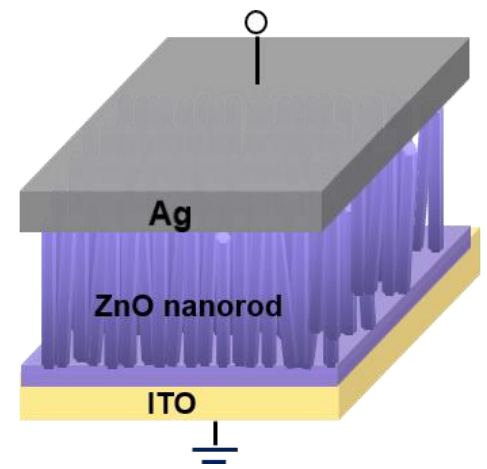
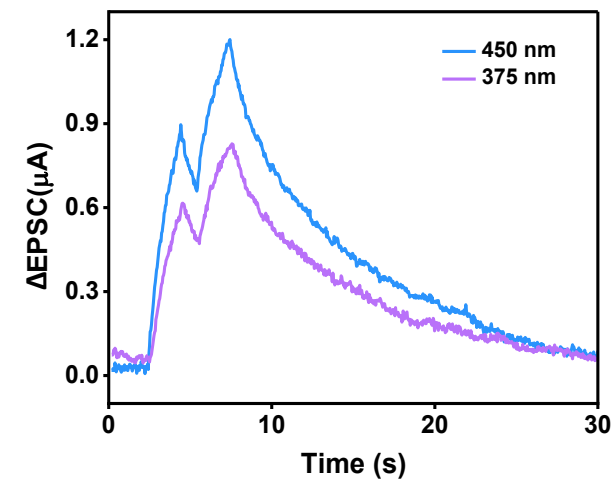
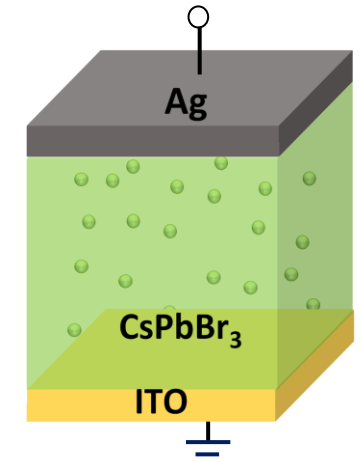


Excitatory & Inhibitory-synaptic behaviour



❖ Positive photo-conductance (PPC) for 375 nm and negative photo-conductance (NPC) for 450 nm light pulses.

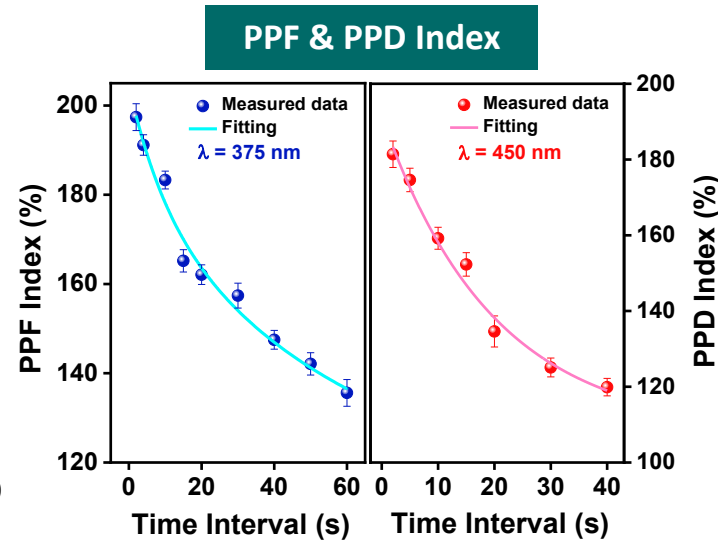
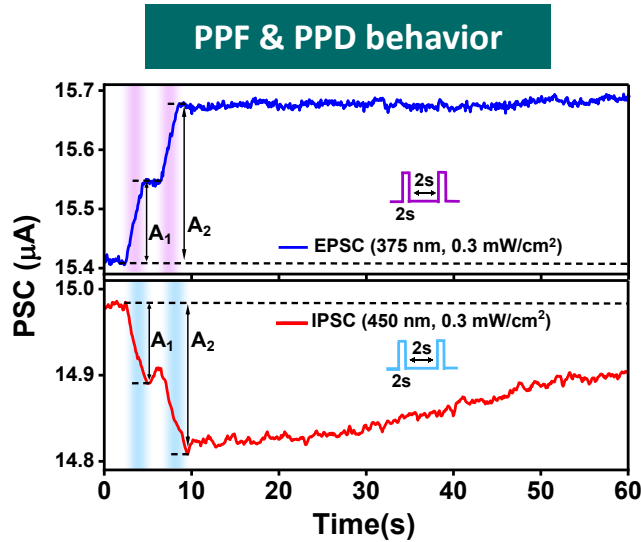
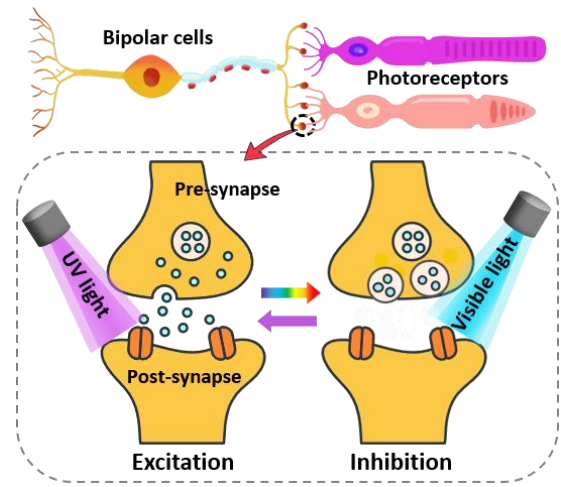
Control Devices



❖ CsPbBr₃-only devices show PPC nature in all wavelengths.
 ❖ ZnO-only devices show PPC nature in 375 nm but show negligible response in 450 nm wavelength.

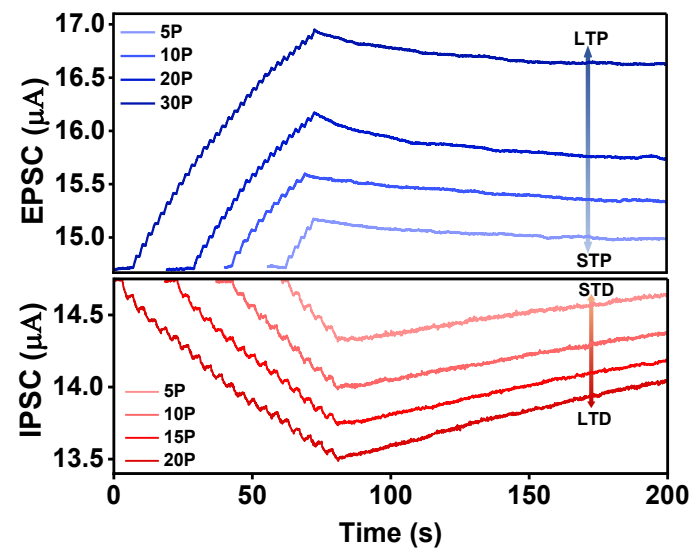


Mimicking fully light-controlled Excitatory & Inhibitory Synapses

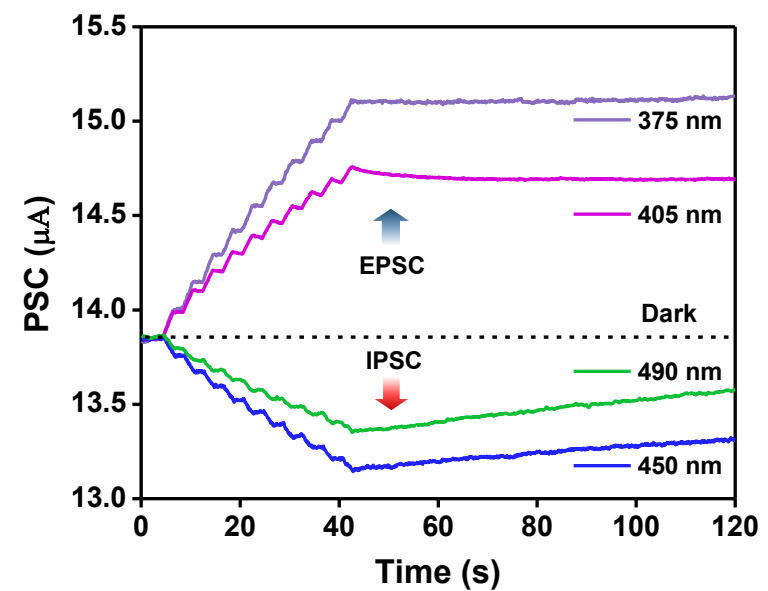


- $PPF (\%) = \frac{A_2}{A_1} \times 100 = C_1 e^{-\frac{t}{\tau_1}} + C_2 e^{-\frac{t}{\tau_2}} + C_3$
- A_1 is post-synaptic response due to the first spike and A_2 due to the second spike, τ_1 and τ_2 are characteristic time constants.
- Highest PPF index is 197.6% and highest PPD index 181.4% for 500 ms interval.

Spike Number-Dependent Plasticity



Wavelength-Dependent Plasticity

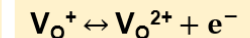
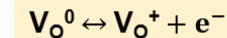
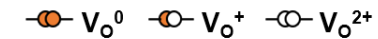
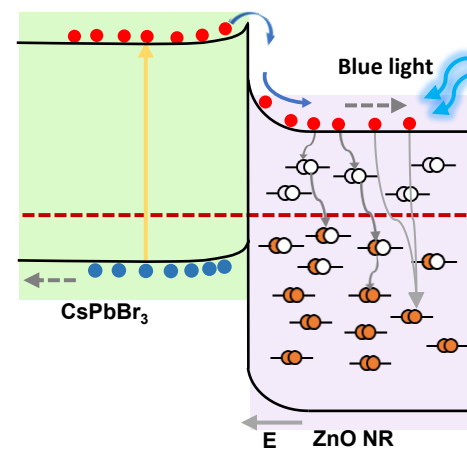
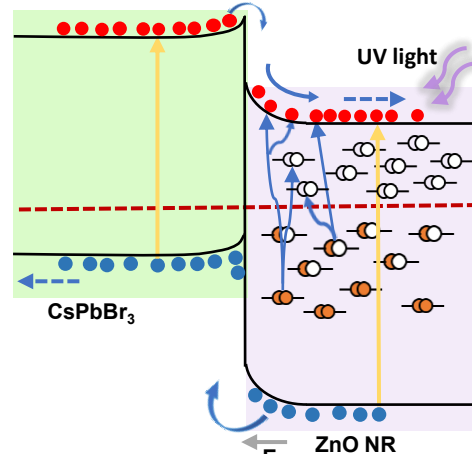
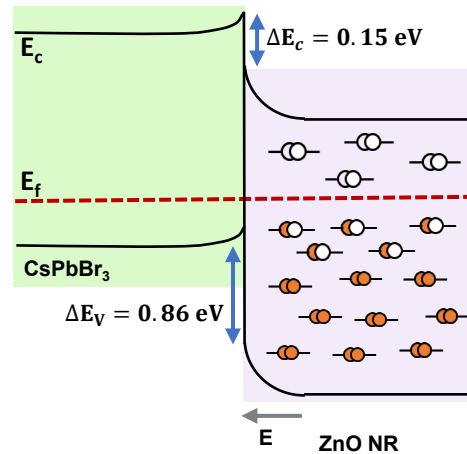
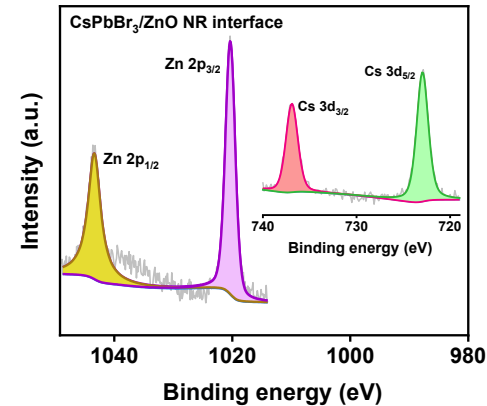
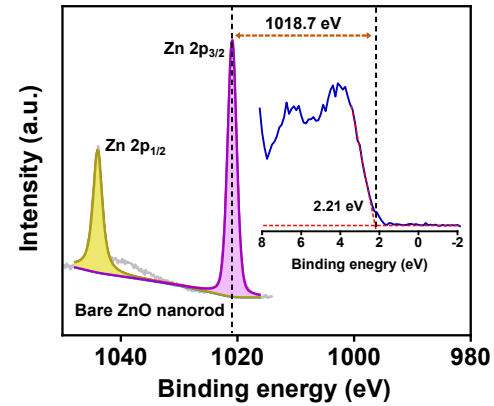
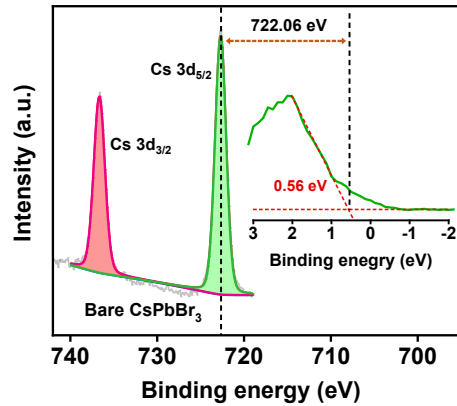


- Both excitatory and inhibitory response strength increase with number of spikes : a transition from short-term memory (STM) to long-term memory (LTM)
- Exhibits an excitatory response under 375 nm and 405 nm excitation and inhibitory responses for both 450 nm and 490 nm illumination
- Energy consumption (E) per spiking event $\sim 72.5 \text{ nJ}$ using $E = V \cdot I \cdot t$, V is the read voltage, t the optical pulse width, and I is the triggered current

Communicated..



Mechanism for bidirectional photoresponse



After contact

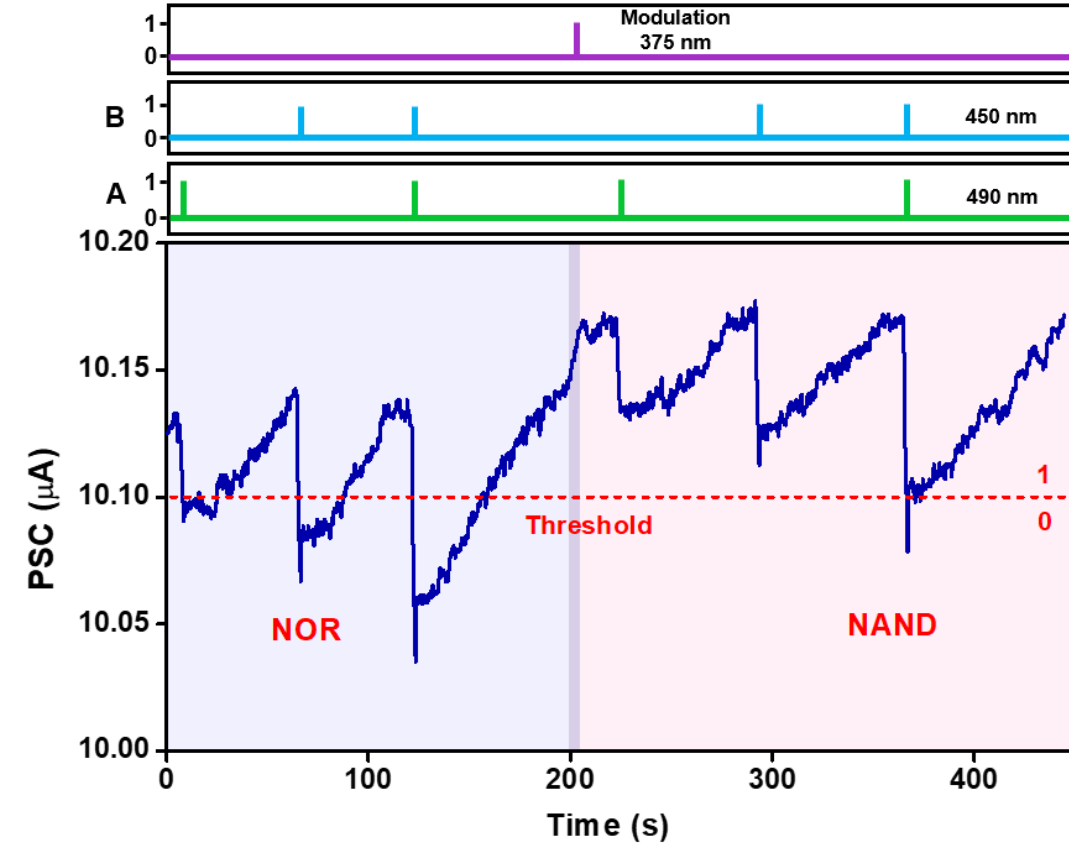
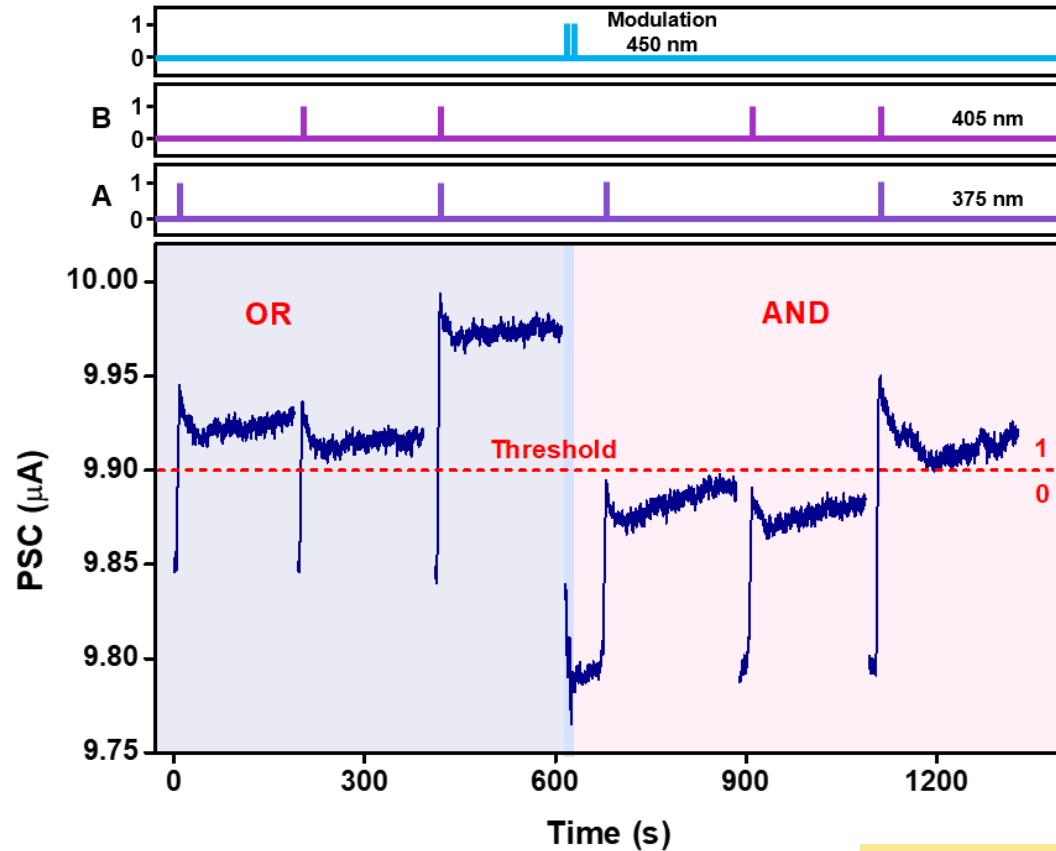
Under UV illumination

Under blue illumination

- ❖ Upon UV (375 nm) excitation, photoionization of insulating α -type ground-state oxygen vacancies (V_o) forms metastable conducting β -type doubly-ionized oxygen vacancies (V_o^{2+}), releasing electrons – leading to PPC.
- ❖ Upon Blue light excitation (450 nm), electron-hole pairs generated primarily in CsPbBr3 are captured by the doubly ionized oxygen vacancies and are deionized and return to the ground state, reducing effective charge carriers, leading to NPC effect.



Optical Logic Gate using Bidirectional Photoconductance



Optical input		Logic output			
A	B	OR	AND	NOR	NAND
0	0	0	0	1	1
0	1	1	0	0	1
1	0	1	0	0	1
1	1	1	1	0	0

- ❖ Optical Logic gates OR, AND, NOR, and NAND implemented using the bidirectional photo response.
- ❖ To realize OR and AND Logic, 375 nm and 405 nm pulses were used as inputs, and 450 nm light was used for modulation.
- ❖ To realize NOR and NAND Logic, 375 nm and 405 nm pulses were used as inputs, and 450 nm light was used for modulation.
- ❖ Switched from OR to AND (NPC) and NOR to NAND (PPC) : modulation signal



Conclusion

- Heterogeneous integration : 2D WS₂ & CsPbI₃ – High performance phototransistor
- Demonstrated moderate efficiency CsPbI₃ nanocrystals sensitized solar cells
- Engineered R-P faults in MHP : Tunable & Improved LEDs
- Optoelectronic Synapses – interface engineering to demonstrate both NPC & PPC using same material platform. Artificial vision systems, switchable optical logic gates with PPC & NPC



Acknowledgements



Arup Ghorai
North Carolina State University



Somentah Mahato
Łukasiewicz, Poland

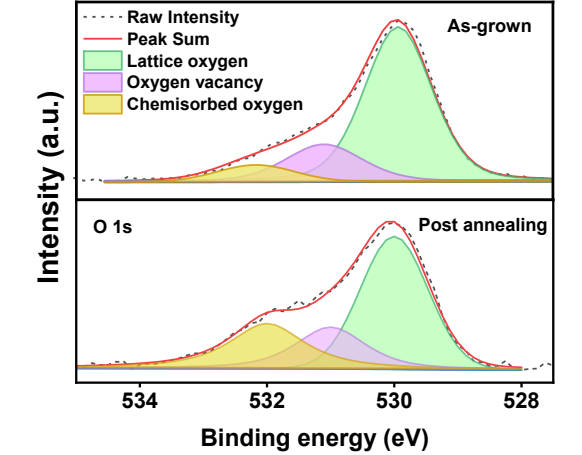
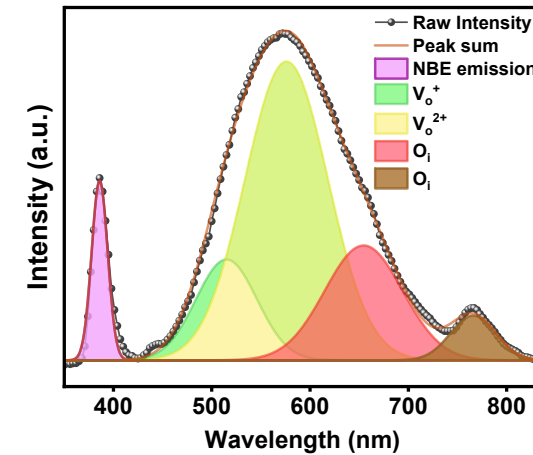
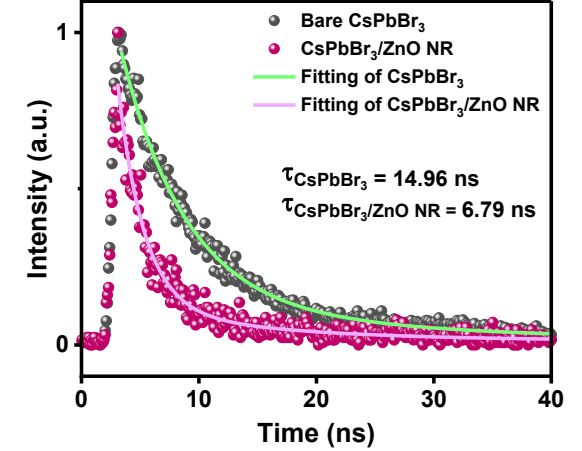
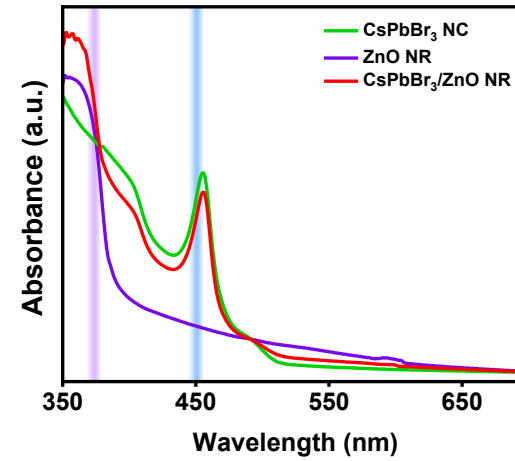
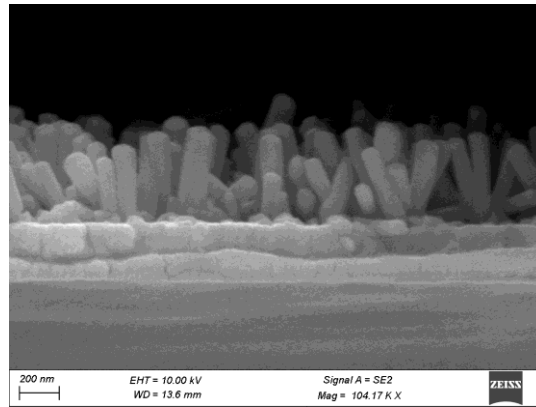
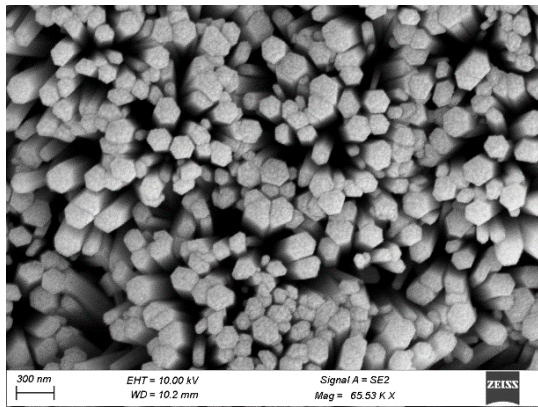
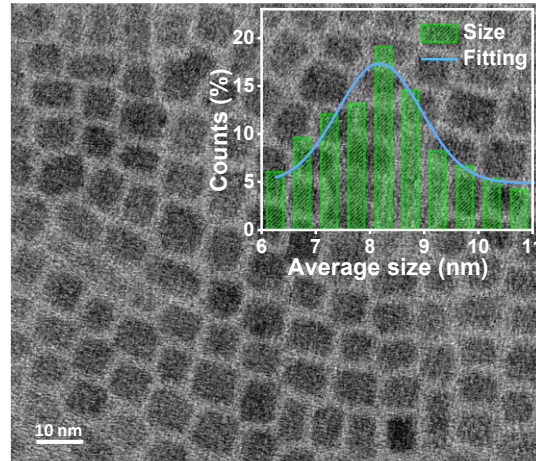
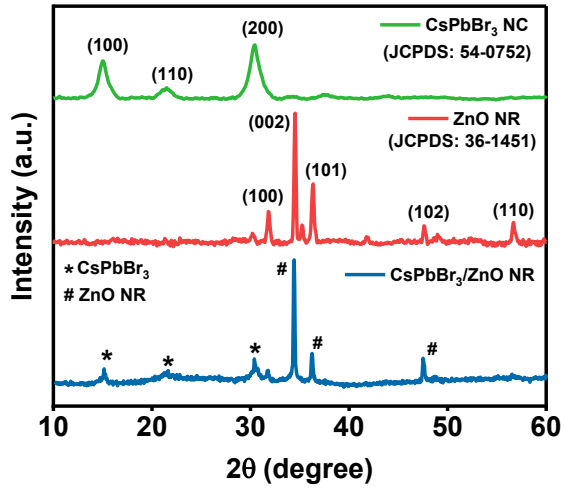


Shreyasi Das, ISTA, Austria



Perovskite-Oxide Heterojunction for All-Optical Synapse

Materials Characterization



- XRD pattern reveals cubic phase of CsPbBr₃ nanocrystals and hexagonal wurtzite phase of ZnO with the nanorods being oriented along the c-axis.
- The average size of the synthesized CsPbBr₃ nanocrystals are ~ 8 ± 1 nm.
- Average length of ZnO nanorods ~450 nm and average diameter ~ 150 nm, calculated from the FESEM images.

- UV-Vis absorption spectra reveal a bandgap of 2.47 eV for CsPbBr₃, 3.2 eV for ZnO nanorods.
- ZnO nanorod room temperature PL spectra reveal different defect peaks (V_o, O_i).
- XPS spectra reveal that ambient annealing reduces the oxygen vacancy concentration and increases the chemisorbed oxygen content.